KEK-TH-1224

arXiv:0905.1453v2 [hep-ph] 5 Sep 2009

Novel two-to-three hard hadronic processes and possible studies of generalized parton distributions at hadron facilities

S. Kumano,[1,2] M. Strikman,[3] and K. Sudoh[1,4]
[1]Institute of Particle and Nuclear Studies
High Energy Accelerator Research Organization (KEK)
1-1, Ooho, Tsukuba, Ibaraki, 305-0801, Japan
[2]Department of Particle and Nuclear Studies
Graduate University for Advanced Studies
1-1, Ooho, Tsukuba, Ibaraki, 305-0801, Japan
[3]Department of Physics, Pennsylvania State University
University Park, PA 16802, U.S.A.
[4]Nishogakusha University, 6-16, Sanbancho, Chiyoda, Tokyo, 102-8336, Japan

(Dated: September 4, 2009)

We consider a novel class of hard branching hadronic processes $a+b \to c+d+e$, where hadrons c and d have large and nearly opposite transverse momenta and large invariant energy which is a finite fraction of the total invariant energy. We use color transparency logic to argue that these processes can be used to study quark generalized parton distributions (GPDs) for baryons and mesons in hadron collisions hence complementing and adding to the studies of GPDs in the exclusive DIS (deep inelastic scattering) processes. We propose that a number of GPDs can be investigated in hadron facilities such as J-PARC (Japan Proton Accelerator Research Complex) facility and GSI-FAIR (Gesellschaft für Schwerionenforschung -Facility for Antiproton and Ion Research) project. In this work, the GPDs for the nucleon and for the $N \to \Delta$ transition are studied in the reaction $N + N \to N + \pi + B$, where N, π, and B are a nucleon, a pion, and a baryon (nucleon or Δ), respectively, with a large momentum transfer between B (or π) and the incident nucleon. In particular, the Efremov-Radyushkin-Brodsky-Lepage (ERBL) region of the GPDs can be measured in such exclusive reactions. We estimate the cross section of the processes $N+N \to N+\pi+B$ by using current models for relevant GPDs and information about large angle πN reactions. We find that it will be feasible to measure these cross sections at the high-energy hadron facilities, and get novel information about the nucleon structure, for example, contributions of quark orbital angular momenta to the nucleon spin. The studies of $N \to \Delta$ transition GPDs could be valuable also for investigating electromagnetic properties of the transition.

PACS numbers: 13.85.-t, 13.60.Le, 12.38.-t

I. INTRODUCTION

Understanding complexity of the structure of hadrons is one of prime objectives of QCD (Quantum Chromodynamics). For a long time, the main focus was the study of single parton densities in inclusive processes for which QCD factorization theorem is valid [1]. More recently, many investigations started to focus on nucleon spin structure by polarized lepton-nucleon scattering and proton-proton collisions. It became clear that only a small fraction (20−30 %) of nucleon spin is carried by quarks [2]. There are still a large uncertainty in the gluon spin contribution [2]; however, recent measurements indicate a tendency that it is also small in the region of momentum fraction $x \sim 0.1$ [3]. It is, therefore, important to find a contribution from orbital angular momenta as a possible source for explaining the nucleon spin.

A parallel development of the last two decades was realization that the QCD factorization theorem is valid for deeply virtual Compton scattering [4] and for exclusive production of mesons in deep inelastic scattering (DIS) by longitudinally polarized photons [5, 6]. Amplitudes of these processes are expressed through universal objects - generalized parton distributions (GPDs) which contain information about both longitudinal and transverse distributions of hadrons.

In the forward scattering limit, several GPDs become usual parton distribution functions with the transverse momentum dependence connected to the transverse coordinate distribution of partons in the hadron [7]. Therefore, studies of GPDs allow to establish the three-dimensional image of the nucleon and hence provide critical information for description of nucleon-nucleon collisions at collider energies [8]. The first moments of GPDs are given by the corresponding hadron form factors providing a link between high-energy and medium-energy dynamics. At the same time the second moment of a certain combination of GPDs is related to the total angular momentum contribution to the nucleon spin and hence probes orbital angular momentum effects in the spin structure of nucleon [9].

For the recent reviews of the properties of GPDs and applications to the study of the hard exclusive DIS processes, we refer the reader to Refs. [10, 11]. Several theoretical calculations have been performed [12, 13, 14, 15, 16, 17] and we will use the ones described in Ref. [12]. Experimental studies of GPDs are performed at HERA (Hadron-Elektron-Ringanlage) collider and in several fixed target experiments [18, 19]. It was also proposed to study GPDs in the $\pi N \to \mu^+\mu^- + N$ process [20].

The QCD factorization theorem for exclusive hard processes induced by longitudinally polarized photons is valid for any exclusive final states in particular exclusive meson production [6]. Hence, one can probe various non-diagonal transitions between baryons - transitional GPDs [21]. For example, the GPDs for the $N \to \Delta$ transition, where N and Δ indicate the nucleon and $\Delta(1232)$, should be important for the studies of nucleon spin [21]. There is also an important link to the $N \to \Delta$ transitional electromagnetic form factors, which are studies in the low-energy electron experiments [22]. Electromagnetic moments of unstable particles such as the Δ cannot be measured by usual methods for stable nuclei [23]. Electromagnetic moments for the $N \to \Delta$ are interesting quantities [22]. In particular, the C2 and E2 transition moments indicate shape deformations of the nucleon and Δ, so that they are valuable for proving interesting information on quark-gluon dynamics [24]. The $N \to \Delta$ GPDs are related to the nucleonic GPDs according to a chiral-quark soliton model in the large N_c limit [10, 21], where N_c is the number of colors. Using the relation to the nucleonic GPDs, we could learn about contributions of quark orbital angular momenta to the nucleon spin.

It was suggested in Refs. [25, 26] that one can investigate presence of small-size color singlet $q\bar{q}$ and qqq clusters in hadrons using large-angle branching hadronic processes $a + b \to c + d + e$ where the hadron e is produced in the fragmentation of b with fixed Feynman x_F and fixed transverse momentum $p_T^{(e)}$, while the hadrons c and d are produced with large and near balancing transverse momenta: $p_T^{(c)} \approx -p_T^{(d)}$.

In this paper, we will argue that investigations of these processes allow to probe various diagonal and transitional GPDs of hadrons. We will focus on one of the simplest subclass of these reactions $N + N \to N + \pi + B$, where π indicates the pion and B does the nucleon or Δ. We will argue that these reactions allow to probe the GPDs for the nucleon and the $N \to \Delta$ transition in the kinematical region of Efremov-Radyushkin-Brodsky-Lepage (ERBL) [27] at hadron facilities in addition to the lepton scattering measurements. Especially, there are future projects such as the J-PARC (Japan Proton Accelerator Research Complex) facility [28] and GSI-FAIR (Gesellschaft für Schwerionenforschung -Facility for Antiproton and Ion Research) project [29] for investigating high-energy proton and anti-proton reactions. Other branching reactions which one can study at these facilities include reactions initiated by meson projectiles which provide a unique way to probe meson GPDs: $\pi + N \to \pi + \pi +$ low-p_T baryon and processes initiated by protons (antiprotons) involving production of two large angle baryons (baryon and antibaryon at the GSI-FAIR) with a small transverse momentum for the pion: $p(\bar{p}) + N \to p(\bar{p}) + N +$ low-p_T meson. The cross sections of the processes with two large transverse momentum baryons are expressed by skewed (transitional) parton distributions $N \to M$ [26], where M indicates a meson. Experimental indications for existence of back to back production of two protons with large p_t were reported in Ref. [30].

This article is organized as follows. In Sec. II, we provide arguments for validity of factorization for *two* $\to$ *three* process and introduce the description of the $N + N \to N + \pi + B$ cross section in terms of a $N \to B$ amplitude and a meson-nucleon scattering part. The GPDs for the nucleon and the $N \to \Delta$ transition are defined and their major properties are introduced in Sec. III. The $N \to B$ amplitude is expressed through the nucleonic or $N \to \Delta$ GPDs in Sec. IV. The meson-nucleon scattering cross sections are parametrized so as to explain experimental measurements in Sec. V. The $N + N \to N + \pi + B$ cross sections are shown in Sec. VI by assuming a J-PARC kinematics for the initial proton and by taking a typical model for the GPDs. The results are summarized in Sec. VII.

II. FACTORIZATION OF CROSS SECTION FOR $\mathbf{N + N \to N + \pi + B}$

It was argued in Ref. [31] that cross sections of large angle scattering processes: $a + b \to c + d$ in the limit of $s \to \infty$ with θ_{cm}=const, where s is the center-of-mass (c.m.) energy squared and θ_{cm} is the scattering angle, are dominated by the short-distance configurations in hadrons both in the initial and final states and satisfy dimensional counting rules. The data on a variety of such processes (see Ref. [32] and references therein) are consistent with the dimensional counting rules. They also indicate that the processes, where quark exchange is allowed, are much larger than those where it is forbidden. The especially interesting is the observed systematics of reactions induced by mesons: the ratio of $K^+p \to K^+p$ and $\pi^+p \to \pi^+p$ cross sections at $\theta_{cm} = 90^o$, where p is the proton, is close to the square of the wave functions K^+ and π^+ mesons at the origin: $[f_K/f_\pi]^2 \approx 1.4$, while it is ~ 0.5 for a small momentum transfer $|t|$.

A test of dominance of the small-size configurations in these processes was suggested by Brodsky and Mueller [33, 34]. They pointed out that since small-size configurations weakly interact with other hadrons the cross section of the large angle processes like $a + A \to a + p + (A - 1)$, where a and A indicate a hadron and a nucleus with mass number A, should be proportional to the number of protons in the nucleus. This regime is usually referred to as the color transparency (CT). The phenomenon which slows down the onset of the CT regime is the space-time evolution of the small wave packages. Evolution occurs over the distance scale l_{coh} (coherence length), which can be estimated as $l_{coh} \sim 0.3 \div 0.4$ fm $\cdot\, p_h$/GeV, where p_h is the hadron momentum [35]. Recently, the color transparency phenomenon was observed in the electroproduction of pions [36] with the change of the transparency consistent with the prediction of Ref. [37], in which above estimate of l_{coh} was used. For the review of the CT phenomena in the high-energy processes, see Ref. [8].

Overall, it appears that there is a good evidence for dominance of the small-size configurations in the large angle meson-nucleon scattering and for suppression of the interaction of small-size configurations near the interaction point. Hence, the meson-nucleon scattering at large angles should be a good probe of short-distance effects already at moderate energies $s_{\pi N} \sim 12$ GeV^2 and large $\theta_{cm} \sim 90^o$. Therefore, we start our investigation of the *two* → *three* processes with the reaction $N + N \to N + \pi + B$ in the kinematics where nucleon scatters at large $|t'|$ off a small-size color singlet $q\bar{q}$ clusters in the nucleon. This is analogous to the process of $\gamma^* + N \to \pi + B$ scattering at $x \geq 0.2$, where dominant contribution originates from the scattering off small-size color singlet $q\bar{q}$ clusters in the nucleon [10]. These processes allow to investigate the nucleonic and $N \to \Delta$ transition GPDs. An additional advantage is that these GPDs are extensively studied in the literature so that we will be able to use existing analyses of these GPDs to perform numerical estimates. In this section, we explain how to calculate the cross section of these reactions and give arguments for validity of the factorization.

The cross section is given by

$$\begin{aligned} d\sigma = & \frac{S}{4\sqrt{(p_a \cdot p_b)^2 - m_N^4}} \overline{\sum_{\lambda_a,\lambda_b}} \sum_{\lambda_d,\lambda_e} |\mathcal{M}_{NN\to N\pi B}|^2 \\ & \times \frac{1}{2E_c}\frac{d^3p_c}{(2\pi)^3}\frac{1}{2E_d}\frac{d^3p_d}{(2\pi)^3}\frac{1}{2E_e}\frac{d^3p_e}{(2\pi)^3} \\ & \times (2\pi)^4\delta^4(p_a + p_b - p_c - p_d - p_e), \end{aligned} \tag{1}$$

where $\mathcal{M}_{NN\to N\pi B}$ is the matrix element for the process $NN \to N\pi B$, m_N is the nucleon mass, and λ_i (i=a, b, d, e) is a spin of an initial or final particle. The factor S is 1/2 if the final baryon is identical to the final nucleon N and it is 1 if they are not identical. The particle indices a, b, c, d, and e are assigned to the initial nucleons and final nucleon, pion, and baryon B (nucleon or Δ) as shown in Fig. 1. Their momenta and energies are denoted as p_i and E_i (i=a, b, c, d, e). Averages are taken for the initial spins λ_a and λ_b. Mandelstam variables s, t, s', and t' are defined

$$\begin{aligned} s = (p_a + p_b)^2, \quad t =& (p_a - p_e)^2, \\ s' = (p_c + p_d)^2, \quad t' =& (p_b - p_d)^2, \end{aligned} \tag{2}$$

for this reaction. Note that two complementary kinematic regions contribute to the discussed cross section. In one kinematics B has small momentum relative to nucleon (a) - the target nucleon, while in the second kinematics t is small relative to the projectile - nucleon (b). These two cross sections are obviously equal. The corresponding amplitudes do not interfere in the discussed limit. Hence for simplicity we will present the results for one kinematics only. At the moment, there exists no procedure for calculating cross sections of N+$N \to N$+π+B process in a generic kinematics. However, it is simplified for the hard regime: $|t'| \gg m_N^2$ and $|u'| = |(p_b - p_c)^2| \gg m_N^2$. Formal arguments can be developed for the limit

$$s' \to \infty, \quad \frac{t'}{s'} = \text{const}, \tag{3}$$

since the leading-order QCD diagrams dominate the cross section of two-body processes [31]. All the partons which experience a large change of the direction have to be attached to hard lines. This idea is used as a counting rule for estimating energy dependence of exclusive cross sections at high energies [31, 38]. In our studies, the variable $|t|$ is fixed and sufficiently small ($|t| \ll m_N^2$), and the center-of-mass energy is $\sqrt{s} \simeq \sqrt{60} \div \sqrt{100}$ GeV at the J-PARC.

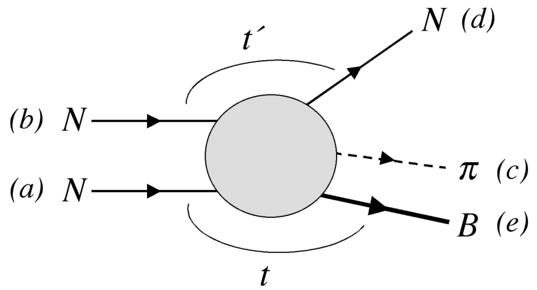

FIG. 1: $N + N \to N + \pi + B$ reaction.

Similar to the logic of the QCD counting rules of Ref. [31], we separate diagrams with minimal number of hard gluons. The hard part of these diagrams has the same topologic structure as the diagrams for the corresponding elementary reaction M+$N \to M'$+B. A typical diagram of this kind is presented in Fig. 2.

It is easy to check that other processes which contribute to the $N + N \to N + \pi + B$ cross section, are

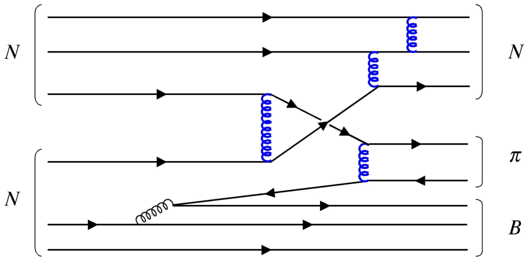

FIG. 2: (Color online) A typical leading subprocess contribution, which corresponds to Fig. 4, to the N+$N \to N$+π+B cross section. The spirals indicate gluon exchanges. The thick spirals show hard gluon exchanges, whereas the narrow one shows a soft gluon exchange. In the large $|t'|$ and $|u'|$ process, the quarks in the final baryon and pion should be attached to the hard gluon lines.

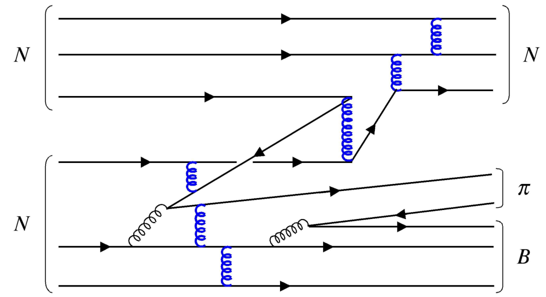

FIG. 3: (Color online) A typical subleading contribution to the $N + N \to N + \pi + \Delta$ cross section. As explained in the text, the nucleon (a) splits as $N \to q\bar{q} + B^* \to \pi + B$, then the $q\bar{q}$ pair interacts with another nucleon (b) ($N + q\bar{q} \to N$). Notations for soft and hard gluons are the same in Fig. 2.

suppressed by powers of s' in the limit of Eq. (3). For example, in the case of a diagram shown in Fig. 3, the process proceeds via $N \to q\bar{q} + B^* \to q\bar{q} + \pi + B$, where B^* indicates an intermediate baryonic state, in the lower blob of this figure and subsequent transition $N + q\bar{q} \to N$ in the upper one. In this case, the amplitude is small because the $q\bar{q}$ propagation is suppressed by the factor $1/|t'|$ ($|t'| \gg m_N^2$), whereas the corresponding factor in Fig. 2 is $1/|t|$ ($|t| \ll m_N^2$). Furthermore, the large momentum ($|t'|$) is also involved in the lower blob ($N \to q\bar{q} + B^*$) in addition to the upper one. It means that more hard gluon exchanges are involved in this case, which suppresses the contribution in Fig. 3.

Next, we need to demonstrate that additional soft interactions, which are not suppressed by powers of t', are canceled out. The easiest way is to consider the process in the rest frame of fragmenting nucleon. Neglecting space-time evolution of the wave packets, which is legitimate in the limit of Eq. (3), we observe that transverse size of the projectile and two outgoing hadrons near the interaction point is given by $\sim 1/\sqrt{|t'|}$. Hence, the color transparency arguments essential for the proof of factorization for exclusive hadron production in DIS [6] are applicable, and the soft interactions are suppressed by at least a power of $1/t'$. Hence, we find that the leading contribution to the $N + N \to N + \pi + B$ amplitude is given by the factorized form.

The transition amplitude $\mathcal{M}_{NN \to N\pi B}$ is written as a convolution of generalized parton distribution $G(N \to B)$ of $q\bar{q}$ pairs in the nucleon with a hard interaction blob H of $q\bar{q}$ - $3q$ elastic scattering and $q\bar{q}$ ($3q$) wave functions of the initial nucleon (b), the final nucleon (d), and (c):

$$\mathcal{M}_{NN \to N\pi B} = G(N \to B) \otimes \psi_N^i \otimes H\psi_\pi \otimes \psi_N^f. \tag{4}$$

Here, $\otimes$ denotes convolution of the different blocks, namely an integration over the light-cone fractions of constituents involved in the process, *etc.* There is also an implicit summation over the intermediate states. We can also rewrite Eq. (4) in somewhat more transparent form as:

$$\mathcal{M}_{NN \to N\pi B} = \mathscr{M}_{N \to hB}\, \mathscr{M}_{hN \to \pi N}, \tag{5}$$

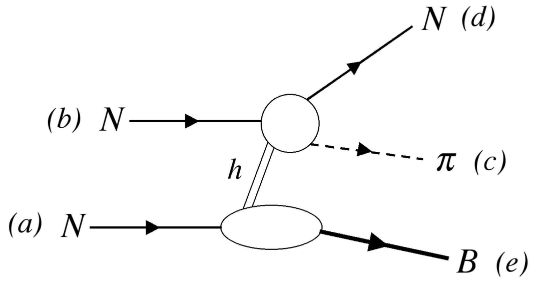

FIG. 4: Factorization of $N + N \to N + \pi + B$ process into $N \to h + B$ and $h + N \to \pi N$ amplitudes.

where h indicates the intermediate $q\bar{q}$ hadronic state and the nucleon, respectively. This corresponds to the diagram of Fig. 4.

Consequently, the cross section has the following generic factorized form in the limit of Eq. (3):

$$\frac{d\sigma}{d\alpha d^2 p_{BT} d\theta_{cm}} = f(\alpha, p_{BT})\phi(s', \theta_{cm}), \tag{6}$$

where α and p_{BT} are the light-cone fraction and transverse momentum carried by B (in the GPD notation $\alpha = (1-\xi)/(1+\xi)$, see section 3). The cross section is separated into the function f (and ϕ) which depends on the variables α and p_{BT} (s' and θ_{cm}). The invariant energy of the subprocess is $s' = (1-\alpha)s$, and the function ϕ is the cross section for the $q\bar{q}$-$3q$ scattering, and it is given by the quark counting rules as $\phi(s', \theta_{cm}) \approx (s')^n \gamma(\theta_{cm})$, where $\gamma(\theta_{cm})$ is a function which depends only on the angle θ_{cm}, and n is the total number of all interacting elementary fields. Phenomenologically, it appears more natural to use for numerical studies of experimental s', t' dependence of the elementary reaction $\pi N \to MN$, where M is a meson, rather than the asymptotic quark counting values.

Note the cross section as given by Eq. (6) does not depend on the direction of the transverse component of the momentum of B, or equivalently the cross section does not depend on the angle between the plane formed by B and the target nucleon and the plane of the hard reaction. This provides an important test of factorization as the rescatterings, which are discussed below, lead to break down of this factorization property.

To determine at what t' we may expect the onset of factorization, we notice that the minimal condition is that qqq and $q\bar{q}$ wave packets, which are small in the interaction point, involved in the hard interaction block should remain small while passing by the spectator system. Hence, the distance over which a small wave package expands or contracts - l_{coh}, should satisfy the condition

$$l_{coh} > r_N \sim 0.8 \text{ fm}, \tag{7}$$

corresponding to expansion of the outgoing hadrons and collapse of incoming proton outside the target proton

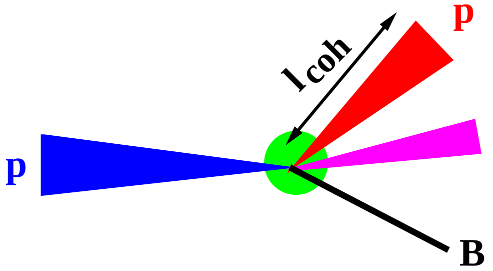

FIG. 5: Time evolution of wave packets of interacting hadrons in the $2 \to 3$ process.

as shown in Fig. 5. Here, 0.8 fm indicates the size of the nucleon. A similar condition exists in the discussion of the color transparency phenomena with nuclei where it is necessary to have $l_{coh} \geq 2R_A$, where R_A is a nuclear radius, to reach the regime of complete color transparency. The studies of the evolution rates of qqq and $q\bar{q}$ wave packets in the framework of the nuclear color transparency have led to the estimates corresponding to (for the review of different models of space-time evolution of wave packages, see Ref. [35])

$$l_{coh} = (0.3 \div 0.4 \text{ fm}) \cdot p_h/(\text{GeV}/c). \tag{8}$$

In the case of pions, it is checked to a large extent by the measurement of the A and Q^2 dependence of transparency in the $A(e, e'\pi)$ reaction [36]. The condition of Eq. (7) is obviously much less stringent than for the case of CT phenomena with nuclei. It corresponds to requirement that final momenta of the two hadrons with large p_T are

$$p_c \geq 3 \div 4 \text{ GeV}/c, \quad p_d \geq 3 \div 4 \text{ GeV}/c, \tag{9}$$

which is satisfied for the incident nucleons with $p_N \geq 8$ GeV/c.

Spins and parities of N and Δ are $\frac{1}{2}^+$ and $\frac{3}{2}^+$, so that the state h should be in 1^+. If it is a p-wave pion- or rho-like state, it is allowed. In general, h could be expressed by the Fock-space expansion, $|h>=|q\bar{q}>+|qq\bar{q}\bar{q}>+\cdots$. However, higher Fock states are suppressed because more hard gluon exchanges are needed to form the final pion and nucleon with large momenta. Therefore, the intermediate state should be considered as a $q\bar{q}$ state. Gluonic states such as gg are excluded as the intermediate state h for $N \to \Delta$ because the isospin state of h should be one by considering isospins of N and Δ are $\frac{1}{2}$ and $\frac{3}{2}$, respectively. They are present for the $B = N$, though the data indicate [32] that contribution of diagrams with gluon exchanges is much smaller than that with quark exchanges.

If the final baryon (B) is a nucleon, there are additional contributions in principle. The same discussions on isospin, spin, and parity suggest that the intermediate state should be in 0^+ and 1^+ states. The 1^+ state is the same as the $N \to \Delta$ case. There is an additional intermediate state with the vacuum quantum number 0^+. Therefore, the Fock-space expansion is $|h>=|gg>+|q\bar{q}>+|qq\bar{q}\bar{q}>+\cdots$. We do not take into account the 0^+ intermediate state in our current work with the following reasons. Lattice QCD calculations indicate that the mass of the lightest 0^+ glueball is estimated about 1700 MeV [39]. Even if they were included in the cross-section estimate, their contributions are not significant in the kinematical region of $|t| \ll m_N^2$ because of their large masses. The $f_0(600)$ (or σ) and $f_0(980)$ mesons are not S-wave $q\bar{q}$ states, so that their contributions are suppressed in the limit $t' \to \infty$ with t'/s'=const as follows. We have a meson-nucleon scattering amplitude which is proportional to the integral of the initial and final meson light-cone waves function over quark momenta: $\int \phi_M(z, \vec{p}_\perp) dz d^2 p_\perp$, where z and $\vec{p}_\perp$ are the lightcone momentum fraction and transverse momentum of a quark, respectively. However, wave functions of mesons which are in the P-wave in the nonrelativistic limit have the property $\phi_M(1-z, \vec{p}_\perp) = -\phi_M(z, \vec{p}_\perp)$ [40], so that the integral vanishes since the final-state meson wave function is symmetric. If the f_0 mesons are tetra-quark ($qq\bar{q}\bar{q}$) or meson-molecule states [41], their contributions are suppressed due to more hard gluon exchanges. In any case, it is possible to take channels, such as $p + p \to p + \pi^+ + n$, where the vacuum-like exchange does not contribute. In this way, we consider only the $q\bar{q}$ state as the intermediate state:

$$h = q\bar{q}. \tag{10}$$

We would like to emphasize here that the practical problem we face is that though it is possible to write the amplitude as a sum of the terms representing convolutions of nucleon (transitional) GPDs with the hard blocks H of the $q\bar{q}$-$3q$ scattering, these blocks are not known so far and hence generic factorized expression is not useful for numerical calculations. Accordingly, we use an observation from the current studies of GPDs that a distribution in the ERBL region over z is to a very good accuracy symmetric and very close to that in the wave functions of π and ρ mesons which are close to the asymptotic form starting with virtualities of a few GeV^2 [10]. This will allow us to use the information about elementary two body reactions.

We explain our description of the nucleon and $N \to \Delta$ transition amplitudes $\mathscr{M}_{N\to hB}$ in terms of the nucleonic and transition GPDs in Sec. IV, and the amplitude $\mathscr{M}_{hN\to\pi N}$ is explained in Sec. V.

III. GENERALIZED PARTON DISTRIBUTIONS FOR NUCLEON AND $N \to \Delta$ TRANSITION

A. Generalized parton distributions for nucleon and $N \to \Delta$ transition

Generalized parton distributions are introduced in the $N \to B$ amplitude for the nucleon and $N \to \Delta$ for transitions with neutral exchange in t-channel ($p \to p$, $p \to \Delta^+$) with other transitions related to these ones by the isospin symmetry. The $N+N \to N+\pi+B$ cross section is factorized into two amplitude in Eq. (5). In this section, the first term $\mathscr{M}_{N\to hB}$ is explained. The intermediate state h should be considered as a $q\bar{q}$ state for a reaction with large-momentum transfer $|t'|$, $|u'| \gg m_N^2$. It is important to note that extraction of such a $q\bar{q}$ state with a light-cone separation is related to the GPDs in the ERBL kinematical region [11, 27]. Therefore, the amplitude $\mathscr{M}_{N\to hB}$ is simply given by $\mathcal{M}_{N\to B}$ times the factor describing a light-like separated $q\bar{q}$ pair.

The GPDs for the nucleon is given by off-forward matrix elements of quark and gluon operators with a light-cone separation between nucleonic states [10, 11]. The matrix element of vector current is associated with unpolarized GPDs for quarks in the nucleon:

$$\begin{aligned}\mathcal{M}_N^V &= \int \frac{d\lambda}{2\pi} e^{i\lambda x} \left\langle N, p_e \left| \overline{\psi}(-\lambda n/2) \not{n} \psi(\lambda n/2) \right| N, p_a \right\rangle \\ &= I_N \, \overline{\psi}_N(p_e) \big[H(x,\xi,t) \, \not{n} + E(x,\xi,t) \frac{i\sigma^{\alpha\beta} n_\alpha \Delta_\beta}{2m_N} \big] \psi_N(p_a),\end{aligned} \tag{11}$$

where I_N is the isospin factor for the nucleon given by $I_N =< 1/2||\widetilde{T}||1/2 > \langle \frac{1}{2} M_N : 1m | \frac{1}{2} M'_N \rangle / \sqrt{2}$ [42]:

$$I_N = 1, \ \sqrt{2} \ \text{ for } p \to p, \ n, \tag{12}$$

$\sigma^{\alpha\beta}$ is defined by $\sigma^{\alpha\beta} = (i/2)[\gamma^\alpha, \gamma^\beta]$, and n^μ is a light-cone null vector which satisfies

$$n^2 = 0, \quad n \cdot P = 1 \ \text{ for } P = \frac{1}{2}(p_a + p_e). \tag{13}$$

The vector n^μ is chosen so as to have $n^+ = \vec{n}_\perp = 0$, where $\vec{n}_\perp$ is the transverse vector and $n^\pm$ is defined by $n^\pm = (n^0 \pm n^3)/\sqrt{2}$. Then, n_-^μ is simply denoted as n^μ in the following discussions [43, 44]:

$$n^\mu \equiv n_-^\mu = \left(\frac{1}{2P^+}, \ 0, \ 0, \ -\frac{1}{2P^+} \right). \tag{14}$$

The momentum P is the average over the initial and final nucleon momenta. The integral variable λ is defined by $\lambda = P \cdot z \simeq P^+ z^-$. In Eq. (11), $\psi(\lambda n/2)$ is the quark field. The functions $H(x,\xi,t)$ and $E(x,\xi,t)$ are the unpolarized GPDs for the nucleon. The Dirac spinor for the nucleon is denoted as $\psi_N(p)$. Quark-spin dependent GPDs are also defined in the similar way for the nucleon:

$$\begin{aligned}\mathcal{M}_N^A &= \int \frac{d\lambda}{2\pi} e^{i\lambda x} \left\langle N, p_e \left| \overline{\psi}(-\lambda n/2) \not{n} \gamma_5 \psi(\lambda n/2) \right| N, p_a \right\rangle \\ &= I_N \, \overline{\psi}_N(p_e) \big[\widetilde{H}(x,\xi,t) \, \not{n} \gamma_5 + \widetilde{E}(x,\xi,t) \frac{n \cdot \Delta \gamma_5}{2m_N} \big] \psi_N(p_a),\end{aligned} \tag{15}$$

where $\widetilde{H}(x,\xi,t)$ and $\widetilde{E}(x,\xi,t)$ are the polarized GPDs for the nucleon.

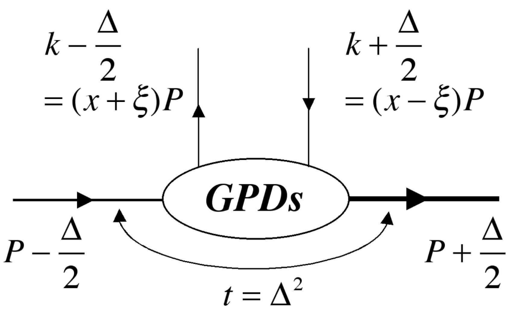

FIG. 6: Kinematics for the $N \to B$ transition and generalized parton distributions.

The generalized scaling variable x and a skewdness parameter ξ are defined in terms of light-cone momentum k^+ ($= (k^0 + k^3)/\sqrt{2}$) and P^+ as

$$k^+ = xP^+, \quad \Delta^+ = -2\xi P^+, \quad \xi = -\frac{1}{2} n \cdot \Delta, \tag{16}$$

where k is the average momentum of the quarks, Δ^μ is the four momentum transfer from the initial nucleon (a) to the final nucleon (e) (or Δ in the $N \to \Delta$ transition), and t is its squared quantity:

$$\Delta = p_e - p_a, \quad t \equiv (p_e - p_a)^2 = \Delta^2. \tag{17}$$

A schematic diagram is illustrated in Fig. 6 for understanding the kinematics of the GPDs. The variable x indicates the momentum fraction carried by a quark in the nucleon as usually used in parton distribution functions (PDFs). The skewdness parameter ξ or the momentum Δ indicates the momentum transfer from the initial nucleon to the final one or the one between the quarks. In the forward limit ($\Delta \to 0$), the nucleonic GPDs $H(x,\xi,t)$ and $\widetilde{H}(x,\xi,t)$ become usual PDFs for the nucleon as shown in Sec. III B.

Next, we explain how to express the transition amplitude $\mathcal{M}_{N\to\Delta}$ in terms of the transition GPDs for $N \to \Delta$. First, the $N \to \Delta$ spin-independent quark distributions are defined by a product of quark fields at a light-cone separation between nucleon and Δ states [10]:

$$\begin{aligned}\mathcal{M}_{N\to\Delta}^V &= \int \frac{d\lambda}{2\pi} e^{i\lambda x} \left\langle \Delta, p_e \left| \overline{\psi}(-\lambda n/2) \not{n} \psi(\lambda n/2) \right| N, p_a \right\rangle \\ &= I_{\Delta N} \overline{\psi}_\Delta^\mu(p_e) \big[H_M(x,\xi,t) \mathcal{K}_{\mu\nu}^M n^\nu + H_E(x,\xi,t) \mathcal{K}_{\mu\nu}^E n^\nu \\ &\qquad + H_C(x,\xi,t) \mathcal{K}_{\mu\nu}^C n^\nu \big] \psi_N(p_a),\end{aligned} \tag{18}$$

where $I_{\Delta N}$ is the $N \to \Delta$ transition isospin factor. The terms $\mathcal{K}_{\mu\nu}^M$, $\mathcal{K}_{\mu\nu}^E$, and $\mathcal{K}_{\mu\nu}^C$ indicate covariants associated with magnetic dipole, electric quadrupole, and Coulomb

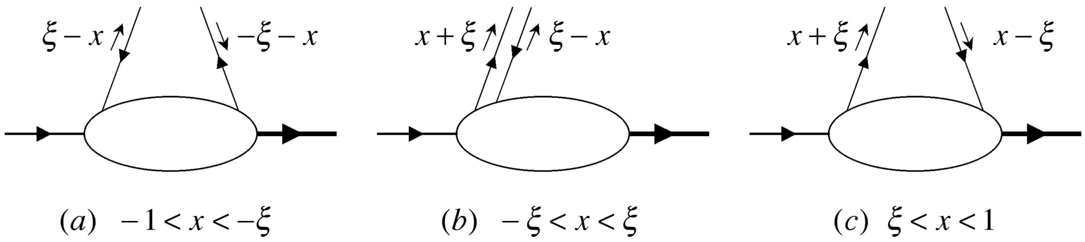

$(a)\ \ -1 < x < -\xi$ $(b)\ \ -\xi < x < \xi$ $(c)\ \ \xi < x < 1$

FIG. 7: Three regions of x for the GPDs: (a) $-1 < x < -\xi$, emission and reabsorption of an antiquark, (b) $-\xi < x < \xi$, emissions of a quark and an antiquark, (c) $\xi < x < 1$, emission and reabsorption of a quark.

quadrupole transitions [45]:

$$\begin{aligned}
\mathcal{K}^M_{\mu\nu} &= -i\frac{3(m_\Delta + m_N)}{2m_N[(m_\Delta + m_N)^2 - t]}\varepsilon_{\mu\nu\lambda\sigma}P^\lambda\Delta^\sigma, \\
\mathcal{K}^E_{\mu\nu} &= -\mathcal{K}^M_{\mu\nu} - \frac{6(m_\Delta + m_N)}{m_N Z(t)}\varepsilon_{\mu\sigma\lambda\rho}P^\lambda\Delta^\rho\varepsilon^\sigma_{\nu\kappa\delta}P^\kappa\Delta^\delta\gamma^5, \\
\mathcal{K}^C_{\mu\nu} &= -i\frac{3(m_\Delta + m_N)}{m_N Z(t)}\Delta_\mu(tP_\nu - \Delta\cdot P\Delta_\nu)\gamma^5, \qquad (19)
\end{aligned}$$

where m_Δ is the Δ mass, and $Z(t)$ is defined by

$$Z(t) = [(m_\Delta + m_N)^2 - t][(m_\Delta - m_N)^2 - t]. \qquad (20)$$

Our conventions for the antisymmetric tensor $\varepsilon_{\beta\mu\lambda\sigma}$ and γ^5 are taken as $\varepsilon_{0123} = +1$ and $\gamma^5 = i\gamma_0\gamma_1\gamma_2\gamma_3$ [10, 11, 46]. The Rarita-Schwinger spinor [47] for the Δ is denoted as $\psi^\mu_\Delta(p)$.

The isospin factor $I_{\Delta N}$ in Eq. (18) comes from the transition isospin. The $N \to \Delta$ transition isospin is define by [42]

$$\left\langle \frac{3}{2}M_\Delta \middle| \widetilde{T} \middle| \frac{1}{2}M_N \right\rangle = \sum_m \frac{1}{2}\left\langle \frac{3}{2} \middle|\middle| \widetilde{T} \middle|\middle| \frac{1}{2} \right\rangle \times \left\langle \frac{1}{2}M_N : 1m \middle| \frac{3}{2}M_\Delta \right\rangle \tilde{\varepsilon}_m, \qquad (21)$$

where $\tilde{\varepsilon}_m$ is the spherical unit vector, $< 3/2||\widetilde{T}||1/2 >= 2$ is a reduced matrix element, and $< 1/2\,M_N : 1\,m|3/2\,M_\Delta >$ is a Clebsch-Gordan coefficient. The isospin factor becomes

$$I_{\Delta N} = 1,\ \sqrt{\frac{2}{3}},\ \sqrt{\frac{1}{3}},\ 0 \ \text{ for } p \to \Delta^{++}, \Delta^+,\ \Delta^0,\ \Delta^-, \qquad (22)$$

respectively.

In Eq. (18), the functions $H_M(x,\xi,t)$, $H_E(x,\xi,t)$, and $H_C(x,\xi,t)$ are the unpolarized GPDs for the transition $N \to \Delta$. Quark-spin dependent GPDs are defined in the same way [10]:

$$\begin{aligned}
\mathcal{M}^A_{N\to\Delta} &= \int \frac{d\lambda}{2\pi}e^{i\lambda x}\left\langle \Delta, p_e \left| \overline{\psi}(-\lambda n/2)\not{n}\gamma^5\psi(\lambda n/2) \right| N, p_a \right\rangle \\
&= I_{\Delta N}\,\overline{\psi}^\mu_\Delta(p_e)\Bigg[\widetilde{H}_1(x,\xi,t)n_\mu + \widetilde{H}_2(x,\xi,t)\frac{\Delta_\mu(n\cdot\Delta)}{m_N^2} \\
&\quad + \widetilde{H}_3(x,\xi,t)\frac{n_\mu\not{\Delta} - \Delta_\mu\not{n}}{m_N} \\
&\quad + \widetilde{H}_4(x,\xi,t)\frac{P\cdot\Delta n_\mu - 2\Delta_\mu}{m_N^2}\Bigg]\psi_N(p_a), \qquad (23)
\end{aligned}$$

where the functions $\widetilde{H}_i(x,\xi,t)$ (i=1, 2, 3, or 4) [48] are the polarized GPDs for the $N \to \Delta$ transition.

Partonic interpretation of the GPDs is different depending on x regions as illustrated in Fig. 7. The x variable is divided into three regions, $-1 < x < -\xi$, $-\xi < x < \xi$, and $\xi < x < 1$, and the GPDs are interpreted as follows in each x region [11]:

(a) "Antiquark distribution"
  $-1 < x < -\xi$ $\ (x+\xi < 0, x-\xi < 0)$
  - Emission of antiquark with momentum fraction $\xi - x$
  - Absorption of antiquark with momentum fraction $-x-\xi$

  Both momentum fractions $x+\xi$ and $x-\xi$ are negative, so that an emission (absorption) of a quark with the negative momentum fraction $x+\xi$ $(x-\xi)$ corresponds to an absorption (emission) of an antiquark with the positive momentum fraction $-x-\xi$ $(-x+\xi)$.

(b) "Meson (quark-antiquark) distribution amplitude"

  $-\xi < x < \xi$ $\ (x+\xi > 0, x-\xi < 0)$
  - Emission of quark with momentum fraction $x+\xi$

  - Emission of antiquark with momentum fraction $\xi - x$

  The momentum fraction $x-\xi$ is negative, so that an absorption of a quark with the negative momentum fraction $x-\xi$ corresponds to an emission of an antiquark with the positive momentum fraction $-x+\xi$.

(c) "Quark distribution"
$\xi < x < 1$ $(x+\xi > 0, x-\xi > 0)$
- Emission of quark with momentum fraction $x+\xi$
- Absorption of quark with momentum fraction $x-\xi$

The regions (a) and (c) are called as DGLAP (Dokshitzer-Gribov-Lipatov-Altarelli-Parisi) regions, and (b) is called the ERBL region [27] depending on evolution types.

If the reaction $N \to h(q\bar{q}) + \Delta$ in Fig. 4 is dominated by the kinematical region $-\xi < x < \xi$, the cross section of $p + p \to p + \pi + \Delta$ should be expressed by the transition GPDs for $N \to \Delta$. They correspond to the distributions in the kinematical region (b) in Fig. 7. The GPDs for the nucleon are calculated, for example, in a chiral soliton model, and results indicated that the GPDs are dominated by a meson-pole contribution at small momentum transfer and that the distributions are located dominantly in the region $-\xi < x < \xi$ [49]. This supports our treatment of the blok $N \to h(q\bar{q}) + \Delta$, in the calculation of the process $N + N \to N + \pi + \Delta$, in terms of the transition GPDs.

B. Properties of generalized parton distributions for nucleon

Here we introduce basic properties of the GPDs for the nucleon. In the forward limit ($\xi = t = 0$), the GPDs H and $\widetilde{H}$ for quarks are given by

$$H(x,0,0) = q(x), \quad \widetilde{H}(x,0,0) = \Delta q(x). \qquad (24)$$

where $q(x)$ and $\Delta q(x)$ are unpolarized and polarized parton distribution functions in the nucleon. Next, their first moments are the form factors of the nucleon:

$$\int_{-1}^{1} dx H(x,\xi,t) = F_1(t), \ \int_{-1}^{1} dx E(x,\xi,t) = F_2(t),$$
$$\int_{-1}^{1} dx \widetilde{H}(x,\xi,t) = g_A(t), \ \int_{-1}^{1} dx \widetilde{E}(x,\xi,t) = g_P(t), \quad (25)$$

where $F_1(t)$, $F_2(t)$, $g_A(t)$, and $g_P(t)$ are Dirac, Pauli, axial, and pseudoscalar form factors of the nucleon. A second moment gives a quark orbital-angular-momentum contribution (L_q) to the nucleon spin:

$$\begin{aligned} J_q &= \frac{1}{2}\int dx\, x\, [H(x,\xi,t=0) + E(x,\xi,t=0)] \\ &= \frac{1}{2}\Delta q + L_q, \qquad (26) \end{aligned}$$

where Δq is the quark-spin contribution and J_q is the total angular-momentum of quarks. It indicates that nucleonic GPD studies are important for clarifying the origin of the nucleon spin. As mentioned in the introduction, the quark contribution to the nucleon spin, possibly as well as the gluon one, is small, so that orbital angular momenta play an important role as the origin of the nucleon spin. These facts indicate that the GPDs are important for understanding basic properties of the nucleon from low to high energies.

C. Properties of generalized parton distributions for $N \to \Delta$ transition

In this section, basic properties of the $N \to \Delta$ transition GPDs are explained. First, the first moment of the GPDs corresponds to the $N \to \Delta$ transition form factors [10, 11]:

$$\int_{-1}^{1} dx H_i(x,\xi,t) = 2G_i(t), \quad i = M,\ E,\ C \qquad (27)$$

where $G_M(t)$, $G_E(t)$, and $G_C(t)$ are the magnetic dipole, electric quadrupole, and Coulomb quadrupole transition form factors, respectively. The $N \to \Delta$ transition is dominated by the M1 transition; however, there are also small E2 and C2 contributions [22, 24]. Experimental investigations have been done in electron scattering, particularly in the processes such as $(e, e'\pi)$ [22, 24, 50]. The E2 and C2 transitions are especially important for investigating a dynamical aspect of baryon structure because they are related to the deformation of the nucleon and Δ. It is interesting to note that information on such a deformation should be also contained in the GPDs. The studies of the $N \to \Delta$ transition GPDs should be valuable for such a new aspect of low-energy hadron structure.

The first moments of $\widetilde{H}_i(x,\xi,t)$ (i=1, 2, 3, 4) are axial form factors for the $N \to \Delta$ transition:

$$\int_{-1}^{1} dx \widetilde{H}_1(x,\xi,t) = 2\, C_5^A(t), \ \int_{-1}^{1} dx \widetilde{H}_2(x,\xi,t) = 2\, C_6^A(t),$$
$$\int_{-1}^{1} dx \widetilde{H}_3(x,\xi,t) = 2\, C_3^A(t), \ \int_{-1}^{1} dx \widetilde{H}_4(x,\xi,t) = 2\, C_4^A(t), \qquad (28)$$

where $C_i^A(t)$ (i=3, 4, 5, or 6) are the axial form factors in Ref. [51]. These axial form factors were studied in parity-violating electron scattering [52]. These Adler form factors are estimated in various theoretical models [52]. For example, a recent estimation by the chiral perturbation theory indicates that C_3^A and C_4^A vanish in the leading order and they become finite due to higher-order corrections: $|C_3^A(t)|, |C_4^A(t)| \ll 1$ [53].

Next, the $N \to \Delta$ GPD studies are also valuable for understanding the origin of the nucleon spin, especially orbital-angular-momentum effects. As an example, possible connections to the nucleon spin are shown by taking the large N_c limit. In the chiral-soliton model, the $N \to \Delta$ transition GPDs are related to the nucleonic GPDs because both baryons are different rotational states of the same soliton [10]:

$$\begin{aligned} H_M(x,\xi,t) =& \frac{2}{\sqrt{3}}\left[E^u(x,\xi,t) - E^d(x,\xi,t)\right], \\ \widetilde{H}_1(x,\xi,t) =& \sqrt{3}\left[\widetilde{H}^u(x,\xi,t) - \widetilde{H}^d(x,\xi,t)\right], \\ \widetilde{H}_2(x,\xi,t) =& \frac{\sqrt{3}}{4}\left[\widetilde{E}^u(x,\xi,t) - \widetilde{E}^d(x,\xi,t)\right], \\ H_E(x,\xi,t) =& H_C(x,\xi,t) = \widetilde{H}_3(x,\xi,t) \\ =& \widetilde{H}_4(x,\xi,t) = 0, \end{aligned} \tag{29}$$

in the leading order of $1/N_c$ expansion. It is especially noteworthy that the second moment of $H_M(x,\xi,t)$ is related to the isovector part of the angular momentum of the nucleon carried by quarks as

$$\begin{aligned} \lim_{t\to 0, N_c\to\infty} & \int_{-1}^{1} dx\ x H_M(x,\xi,t) \\ &= \frac{2}{\sqrt{3}}\left[2(J^u - J^d) - M_2^u + M_2^d\right], \end{aligned} \tag{30}$$

where

$$M_2^q = \int_0^1 dx\ x\left[q(x) + \bar{q}(x)\right], \tag{31}$$

is a second moment of quark and antiquark distribution. The J^u and J^d indicate total angular momenta carried by u and d quarks, respectively. They are equal to the sum of the spin and orbital angular momentum carried by the quark, as shown in Eq. (26). Equation (30) suggests that the $N \to \Delta$ GPDs should be important for investigating the isovector part the orbital angular momentum, $L^u - L^d$, in the studies of nucleon spin.

IV. $N \to B$ TRANSITIONS IN TERMS OF GENERALIZED PARTON DISTRIBUTIONS

A. Generalized parton distributions for the nucleon

For calculating the unpolarized cross section of $N + N \to N + \pi + N$, spin summations are taken for the nucleons. In this section, the factor describing transition from the initial nucleon (a) to the final one (e) is calculated. We discussed the amplitudes M_N^V and M_N^A, which are described by spin independent and dependent generalized quark distributions. The absolute-value squared of the transition amplitude is given by

$$\sum_{\lambda_N,\lambda_{N'}} |\mathcal{M}_N|^2 = \sum_{\lambda_N,\lambda_{N'}} \left(|\mathcal{M}_N^V|^2 + |\mathcal{M}_N^A|^2\right). \tag{32}$$

It should be noted that there is no interference term if the spin summations are taken over λ_N $(= \lambda_a)$ and $\lambda_{N'}$ $(= \lambda_e)$. The summation of the vector and axial contributions indicate that all the associated $q\bar{q}$ states should be included in calculating the cross section. The calculations are done in the same way as mesonic contributions to antiquark distributions [54].

Using the spin summation of the Dirac spinors, $\sum_{\lambda_N} \psi_N(p)\overline{\psi}_N(p) = \not{p} - m_N$ and Eq. (11) for $\mathcal{M}_N^V$, and then calculating traces, we express the vector part of Eq. (32) in terms of nucleonic GPDs:

$$\begin{aligned} \sum_{\lambda_N,\lambda_{N'}} |\mathcal{M}_N^V|^2 = I_N^2 \Big[& 8(1-\xi^2)\{H(x,\xi,t)\}^2 \\ & + 16\xi^2 H(x,\xi,t)E(x,\xi,t) - \frac{t}{m_N^2}(1+\xi)^2\{E(x,\xi,t)\}^2 \Big]. \end{aligned} \tag{33}$$

In the same way, the axial term is calculated as

$$\begin{aligned} \sum_{\lambda_N,\lambda_{N'}} |\mathcal{M}_N^A|^2 = I_N^2 \Big[& 8(1-\xi^2)\{\widetilde{H}(x,\xi,t)\}^2 \\ & + 18\xi^2 \widetilde{H}(x,\xi,t)\widetilde{E}(x,\xi,t) - \frac{2\,t\,\xi^2}{m_N^2}\{\widetilde{E}(x,\xi,t)\}^2 \Big]. \end{aligned} \tag{34}$$

These expressions are used for calculating the cross section for $N + N \to N + \pi + N$.

B. Generalized parton distributions for the $\mathbf{N \to \Delta}$ transition

The $N \to \Delta$ transition part is calculated in the same way by taking spin summations for the nucleon and the Δ. The $N \to \Delta$ transition was described by the matrix elements $\mathcal{M}_{N\to\Delta}^V$ and $\mathcal{M}_{N\to\Delta}^A$ with the transition GPDs in Sec. III A. Then, absolute-value squared of the transition amplitude is

$$\sum_{\lambda_N,\lambda_\Delta} |\mathcal{M}_{N\to\Delta}|^2 = \sum_{\lambda_N,\lambda_\Delta} \left(|\mathcal{M}_{N\to\Delta}^V|^2 + |\mathcal{M}_{N\to\Delta}^A|^2\right). \tag{35}$$

Because the spin summations are taken over λ_N and λ_Δ, there is no interference term.

In our numerical estimation for the cross section, we use the following approximations. First, the electric quadrupole contributions H_E and H_C should be small as suggested in theoretical and experimental studies in the $N \to \Delta$ transition form factors [22, 24]. Therefore, it is appropriate to assume $H_E(x,\xi,t)$=$H_C(x,\xi,t)$=0 for our first estimation of the cross section if such small effects can be neglected. This is also satisfied in the chiral-soliton model as shown in Eq. (29). Then, the vector amplitude is expressed only by the magnetic term:

$$\mathcal{M}_{N\to\Delta}^V = I_{N\Delta}\overline{\psi}_\Delta^\mu(p_e) H_M(x,\xi,t)\mathcal{K}_{\mu\nu}^M n^\nu \psi_N(p_a). \tag{36}$$

Taking the square of its absolute value and performing spin summations, we obtain

$$\sum_{\lambda_N,\lambda_\Delta} |\mathcal{M}^V_{N\to\Delta}|^2 = -I^2_{N\Delta}\,\{H_M(x,\xi,t)\}^2$$
$$\times\ \mathrm{Tr}\left[\sum_{\lambda_\Delta}\psi^\mu_\Delta(p_e)\overline{\psi}^\alpha_\Delta(p_e)\mathcal{K}^M_{\mu\nu}n^\nu \sum_{\lambda_N}\psi_N(p_a)\overline{\psi}_N(p_a)\mathcal{K}^M_{\alpha\beta}n^\beta\right]. \tag{37}$$

Spin summations of the Rarita-Schwinger spinors are given by [47]

$$\sum_{\lambda_\Delta}\psi^\mu_\Delta(p_e)\overline{\psi}^\alpha_\Delta(p_e) = (\not{p}_e - m_\Delta)$$
$$\times\left(-g^{\mu\alpha} + \frac{1}{3}\gamma^\mu\gamma^\alpha - \frac{p^\mu_e\gamma^\alpha - p^\alpha_e\gamma^\mu}{3m_\Delta} + \frac{2p^\mu_e p^\alpha_e}{3m^2_\Delta}\right), \tag{38}$$

where m_Δ is the Δ mass. We denote the trace part of Eq. (37) as $C_M(\xi,t)$:

$$\sum_{\lambda_N,\lambda_\Delta} |\mathcal{M}^V_{N\to\Delta}|^2 = I^2_{N\Delta}C_M(\xi,t)\{H_M(x,\xi,t)\}^2, \tag{39}$$

and it is calculated by using Eq. (38) as

$$C_M(\xi,t) = 3\,\left[\frac{m_N + m_\Delta}{m_N\{(m_N+m_\Delta)^2 - t\}}\right]^2$$
$$\times\left[t - (m_N+m_\Delta)^2\right]$$
$$\times\left[t(1-\xi^2) + 2\xi(m^2_\Delta - m^2_N) + 2\xi^2(m^2_\Delta + m^2_N)\right]. \tag{40}$$

Similarly, the axial-vector part is given by (neglecting the GPDs $H_3(x,\xi,t)$ and $H_4(x,\xi,t)$ as suggested, for example, by the chiral-soliton model [10, 21] and also by the chiral perturbation theory of the form factors [53]):

$$\mathcal{M}^A_{N\to\Delta} = I_{N\Delta}\,\overline{\psi}^\mu_\Delta(p_e)\left[\tilde{H}_1(x,\xi,t)n_\mu + \tilde{H}_2(x,\xi,t)\frac{\Delta_\mu(n\cdot\Delta)}{m^2_N}\right]\psi_N(p_a). \tag{41}$$

Expressing these amplitudes in terms of the GPDs in Eqs. (36) and (41), we obtain

$$\sum_{\lambda_N,\lambda_\Delta} |\mathcal{M}^A_{N\to\Delta}|^2 = I^2_{N\Delta}\left[C_1(\xi,t)\{\widetilde{H}_1(x,\xi,t)\}^2 + C_2(\xi,t)\{\widetilde{H}_2(x,\xi,t)\}^2 + C_{12}(\xi,t)\widetilde{H}_1(x,\xi,t)\widetilde{H}_2(x,\xi,t)\right], \tag{42}$$

where $C_i(\xi,t)$ are coefficient terms and their explicit forms are

$$C_1(\xi,t) = \frac{4}{3m^2_\Delta}\,(1-\xi)^2\left[(m_\Delta+m_N)^2 - t\right], \tag{43}$$

$$C_2(\xi,t) = \frac{4}{3m^4_N m^2_\Delta}\,\xi^2\left[(m_\Delta+m_N)^2 - t\right] \times\left[-4m^2_\Delta t + (m^2_\Delta - m^2_N + t)^2\right], \tag{44}$$

$$C_{12}(\xi,t) = -\frac{8\xi}{3m^2_N m^2_\Delta}\left[(m_\Delta+m_N)^2 - t\right] \times\left[4m^2_\Delta\xi + (1-\xi)(m^2_\Delta - m^2_N + t)\right]. \tag{45}$$

In this way, the $N \to \Delta$ transition part of the cross section can be calculated using the transition GPDs.

V. hN $\to \pi$N SCATTERING AT LARGE MOMENTUM TRANSFER

A. Intermediate q$\bar{\text{q}}$ and mesons

As explained in Sec.III A, the GPDs are separated into three x regions. If the momentum transfer $|t|$ is small, the GPDs distributed dominantly in the $-\xi < x < \xi$, for example, as suggested in Ref. [49]. The GPDs in the kinematical region, $-\xi < x < \xi$, are the distribution amplitudes with the quark and antiquark emissions with momentum fractions $x+\xi$ and $-x+\xi$, respectively.

In general, all associated $q\bar{q}$ states should contribute to the cross section as we considered the vector- and axial-vector amplitudes. At small $|t| \ll m^2_N$, light-meson-like $q\bar{q}$ pairs contribute mostly to the cross section. The dominant ones are the $q\bar{q}$ state with the pion (ρ) quantum numbers in the axial-vector (vector) amplitude. Then, the $q\bar{q}$ pair could be considered as a pion or ρ state in a small-size configuration and the amplitude is given by the meson ($M = \pi$ or ρ) wave function $\phi_M(z)$, and its normalization is given by the Brodsky-Lepage relation [55, 56]. However, our cross sections are independent of the functional form of this wave function in the region where interpolation of the GPDs by the lowest states is a good approximation (see Sec. VI). The kinematical variable z is the light-cone momentum fraction and it is defined in the following way. The variables x_1 and x_2 indicate momentum fractions carried by a quark and an antiquark, respectively, in the nucleon or the $N \to \Delta$ transition. As indicated in Fig. 6, they are expressed by x and ξ as

$$x_1 = x + \xi, \quad x_2 = -x + \xi. \tag{46}$$

The variable z is the momentum fraction carried by the quark to the total momentum of the quark and antiquark system:

$$z = \frac{x_1}{x_1 + x_2} = \frac{x+\xi}{2\xi}. \tag{47}$$

In the previous section, the $N \to B$ part was calculated in terms of the nucleonic and $N \to \Delta$ transition GPDs, which are associated mainly with the $q\bar{q}$ emission. In the small momentum transfer region ($|t| \ll m_N^2$), the $q\bar{q}$ pair could be considered as a pion or ρ state in a small-size configuration, which next interacts with another proton (b) as shown in Fig. 4. The probability that the $q\bar{q}$ pair forms a meson M is described by the meson wave function in the light-cone coordinates. However, it should be noted that the GPDs at the meson pole effectively contain the wave function of the meson in the point like configuration ($\phi_M(z)$) as indicated, for example, in Ref. [10] as the pion-pole contributions. This factor enters also in the meson-nucleon scattering amplitude, so that this factor should be removed in matching of the GPD description with description in terms of scattering off a meson:

$$\mathscr{M}_{(q\bar{q})_M p \to \pi p} = \mathcal{M}_{Mp \to \pi p} / \phi_M(z), \tag{48}$$

where $(q\bar{q})_M$ is a $q\bar{q}$ state with the quantum numbers of the meson M. The critical point here is the observation of several GPD analyses that z distribution of $q\bar{q}$ pairs in the GPDs is close to that in the pion and rho mesons. The off-shell nature of the $q\bar{q}$-N scattering amplitude can be best seen from $s' = -t' - u' + 2m_N^2 + m_\pi^2 + t$ as compared to the on-shell case of $s' = -t' - u' + 2m_N^2 + m_\pi^2 + m_M^2$, where m_M is the meson mass. However, in the limit Eq. (3), the cross section is a function of the ratio of large variables and so correction goes to zero.

For the spin-dependent GPDs in the axial amplitudes $\mathcal{M}_N^A$ and $\mathcal{M}_{N\to\Delta}^A$, the factors are approximated by the pion wave function as long as the $q\bar{q}$ pair has the same spin structure of the pion. For spin-independent GPDs in the vector amplitudes $\mathcal{M}_N^V$ and $\mathcal{M}_{N\to\Delta}^V$, the factors are related to the ρ meson. In this way, the $N + N \to N + \pi + B$ reaction can be calculated by the $N \to B$ transition part and the $MN \to \pi N$ scattering process:

$$\begin{aligned} \mathcal{M}_{NN \to N\pi B} &= \mathscr{M}_{N \to h(q\bar{q})B} \cdot \mathscr{M}_{h(q\bar{q})N \to \pi N}, \\ &\simeq \mathcal{M}_{N \to B} \cdot \mathcal{M}_{MN \to \pi N} / \phi_M(z), \end{aligned} \tag{49}$$

at small momentum transfer ($|t| \ll m_N^2$).

It is worth noting here that the discussed process is directly sensitive to the dependence of the GPDs on ξ. Dependence on x is integrated over. This is similar to the situation in most of the other exclusive hard processes, for example the reaction $\gamma^* + p \to \pi^+ + n$.

Now, the remaining part is the description of the $M + N \to \pi + N$ scattering.

B. Parametrization of cross section for meson-nucleon elastic scattering

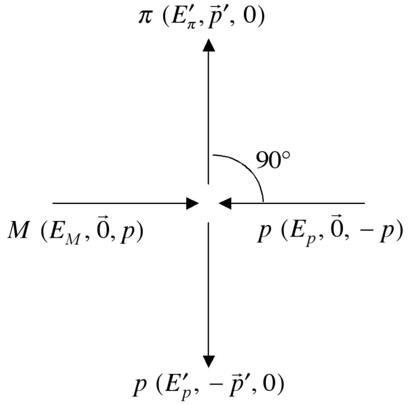

FIG. 8: $Mp \to \pi p$ elastic scattering at $\theta_{c.m.} = 90°$

In order to calculate the cross section of meson-nucleon elastic scattering $Mp \to \pi p$, where p indicates the proton, we try to obtain useful parametrizations of the cross sections by using experimental measurements. The cross section is first expressed in terms of parameters which are then determined by fitting $\pi p \to \pi p$ and $\pi p \to \rho p$ scattering data. The momentum-transfer dependence of the cross section is typically parametrized as [32]

$$\frac{d\sigma_{Mp\to\pi p}(s', t')}{dt'} \propto a + c\,(t' - t'_0)^2, \tag{50}$$

where a and c are parameters, and t'_0 is defined by the t' value at the scattering angle $\theta_{\text{c.m.}} = 90°$ in the center-of-mass (c.m.) system. The Mandelstam variables s' and t' are given in Eq. (2). Moreover, this cross section scales with the c.m. energy squared (s') as

$$\begin{aligned} \frac{d\sigma_{Mp\to\pi p}(s', t')}{dt'} &\sim \frac{1}{s'^{\,n-2}} f_{Mp\to\pi p}(t'/s') \\ &\qquad \text{for } s' \to \infty \ \text{ at fixed } \frac{t'}{s'}, \end{aligned} \tag{51}$$

according to the counting rule [31, 38]. Here, $f_{Mp\to\pi p}(t'/s')$ is a function of t'/s'. The factor n is the total number of all interacting elementary fields, and it is basically the sum of valence-quark numbers in the initial and final states. In the meson-nucleon elastic scattering, $n = 10$ and so the energy dependence is $1/s'^8$.

The factor t'_0 is defined in the c.m. frame, in which our momentum assignment $(E, \vec{p}_T, p_L)$ is shown in Fig. 8. Here, p_T and p_L indicate transverse and longitudinal momenta, respectively. From the energy-momentum conservation, the energies and momenta are given for the mesons and protons as

$$E_M = \frac{s' - (m_p^2 - m_M^2)}{2\sqrt{s'}}, \quad E'_\pi = \frac{s' - (m_p^2 - m_\pi^2)}{2\sqrt{s'}}, \tag{52}$$

$$E_p = \frac{s' + (m_p^2 - m_M^2)}{2\sqrt{s'}}, \quad E'_p = \frac{s' + (m_p^2 - m_\pi^2)}{2\sqrt{s'}}, \tag{53}$$

$$p = \frac{\sqrt{s'^2 - 2s'(m_p^2 + m_M^2) + (m_p^2 - m_M^2)^2}}{2\sqrt{s'}}, \tag{54}$$

$$p' = \frac{\sqrt{s'^2 - 2s'(m_p^2 + m_\pi^2) + (m_p^2 - m_\pi^2)^2}}{2\sqrt{s'}}. \tag{55}$$

TABLE I: Determined parameters in Eq. (57).

Process	Parameters			χ^2/d.o.f.
	a (barn $\cdot$ (GeV)$^{2n-6}$)	c (barn $\cdot$ (GeV)$^{2n-10}$)	$n-2$ (Ref. [32])	
$\pi^+ p \to \pi^+ p$	2.08 ± 0.10	1.11 ± 0.30	6.7 ± 0.2	0.96
$\pi^- p \to \pi^- p$	8.94 ± 0.42	10.46 ± 1.55	7.5 ± 0.3	0.36
$\pi^+ p \to \rho^+ p$	189 ± 14	60.0	8.3 ± 0.5	0.21
$\pi^- p \to \rho^- p$	218 ± 12	200.0	8.7 ± 1.0	0.80

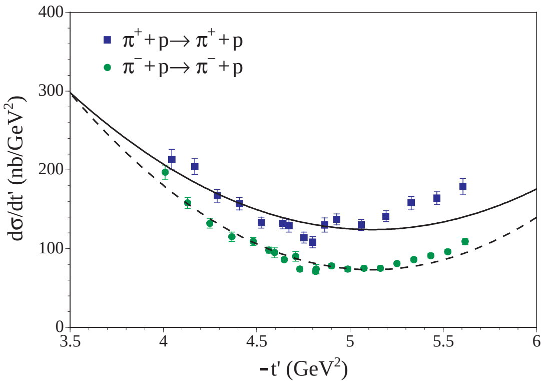

FIG. 9: Data of $\pi^+ p \to \pi^+ p$ and $\pi^- p \to \pi^- p$ cross sections from the BNL-E838 experiment [32] and our parametrization curves of Eq. (57) with the optimized parameters. The solid and dashed curves are for the $\pi^+ p \to \pi^+ p$ and $\pi^- p \to \pi^- p$ cross sections, respectively.

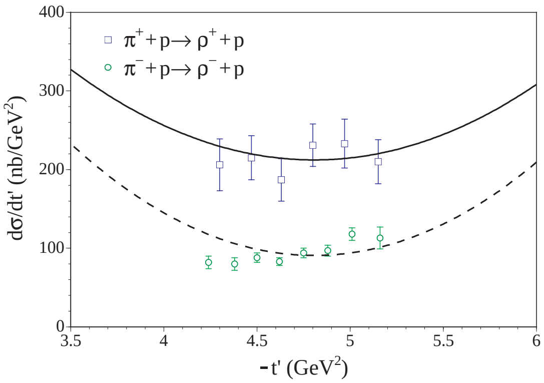

FIG. 10: Data of $\pi^+ p \to \rho^+ p$ and $\pi^- p \to \rho^- p$ cross sections from the BNL-E838 experiment [32] and our parametrization curves of Eq. (57) with the optimized parameters. The solid and dashed curves are for the $\pi^+ p \to \rho^+ p$ and $\pi^- p \to \rho^- p$ cross sections, respectively.

Therefore, t'_0 becomes

$$t'_0 = (p_b - p'_d)^2 \mid_{\theta=\frac{\pi}{2}} \\ = -\frac{s'^2 - s'(2m_p^2 + m_M^2 + m_\pi^2) + (m_p^2 - m_M^2)(m_p^2 - m_\pi^2)}{2s'}. \tag{56}$$

In this way, the differential cross section is parametrized in terms of the variables s' and t' as

$$\frac{d\sigma_{Mp\to\pi p}(s',t')}{dt'} = \frac{1}{s'^{n-2}} \left[a + c(t' - t'_0)^2 \right]. \tag{57}$$

Experimental data are taken from the Alternating Gradient Synchrotron (AGS) experiment E838 [32] with the incident pion-beam 5.9 GeV at the Brookhaven National Laboratory (BNL). They observed large-angle scattering cross sections for $\pi^+ p \to \pi^+ p$, $\pi^- p \to \pi^- p$, $\pi^+ p \to \rho^+ p$, and $\pi^- p \to \rho^- p$. By analyzing the scaling behavior between E755 [57] and E838 data, the parameter $n-2$ was determined as 6.7, 7.5, 8.3, and 8.7 in Ref. [32] as listed in Table I.

We use Eq. (57) for describing the cross sections by the exchange of initial and final states ($Mp \leftrightarrow \pi p$). The parameters a and c are determined by fitting the E838 data. As shown in Figs. 9 and 10, there are 16, 21, 6, 8 data points for $\pi^+ p \to \pi^+ p$, $\pi^- p \to \pi^- p$, $\pi^+ p \to \rho^+ p$, and $\pi^- p \to \rho^- p$, respectively. In Table I, determined parameters are shown and χ^2 values per degrees of freedom are χ^2/d.o.f.=0.96, 0.36, 0.21, and 0.80. The two-parameter fit for the $\pi^\pm p \to \rho^\pm p$ was difficult due to a small number of data. Therefore, the parameter c is fixed at 60 and 200 for $\pi^+ p \to \rho^+ p$ and $\pi^- p \to \rho^- p$, respectively, so as to have similar t-dependency to the $\pi^\pm p \to \pi^\pm p$ cross sections in Fig. 9. The fits are successful in reproducing the data except for some deviations at $t \sim -5.5$ GeV^2 in Fig. 9 and at $t \sim -4.3$ and -5.0 GeV^2 for $\pi^- p \to \rho^- p$ in $\pi^- p \to \rho^- p$ of Fig. 10.

VI. NUMERICAL RESULTS FOR CROSS SECTIONS

A. Expression for $\mathbf{N + N \to N + \pi + B}$ cross section

In this section we calculate the cross sections for the $N + N \to N + \pi + B$ using the parametrizations for the $M + N \to \pi + N$ cross sections, and a model for the nucleonic and $N \to \Delta$ transition GPDs. Here, the expression for the cross section is summarized.

The $MN \to \pi N$ cross section is given by

$$d\sigma_{MN\to\pi N} = \frac{1}{4\sqrt{(p_b \cdot p_M)^2 - m_N^2 p_M^2}} \frac{d^3 p_c}{2E_c (2\pi)^3} \frac{d^3 p_d}{2E_d (2\pi)^3} \\ \times \overline{\sum_{\lambda_b}} \sum_{\lambda_d} |\mathcal{M}_{MN\to\pi N}|^2 (2\pi)^4 \delta^4 (p_b + p_M - p_c - p_d), \tag{58}$$

where $\overline{\sum}_{\lambda_b}$ indicate the average over the initial nucleon (b) spin. The general expression for the cross section is given in Eq. (1) for the process $N+N \to N+\pi+B$. The factor S is $S=1$ in our numerical results for $B=\Delta^0$, Δ^{++}, or neutron, which is not identical to the proton. By assuming the factorization and mesonic $q\bar{q}$ dominance, the matrix-element part is separated into two processes as shown in Eq. (49). Substituting Eq. (49) into Eq. (1), we write the $N+N \to N+\pi+B$ cross section by the $N \to B$ amplitude, namely by the $N \to B$ GPDs, and the $MN \to \pi N$ scattering cross section:

$$d\sigma_{NN \to N\pi B} = \frac{\sqrt{(p_b \cdot p_M)^2 - m_N^2 p_M^2}}{\sqrt{(p_a \cdot p_b)^2 - m_N^4}} \frac{d^3 p_e}{2E_e (2\pi)^3} \times \overline{\sum_{\lambda_a}} \sum_{\lambda_e} \frac{1}{[\phi_M(z)]^2} |\mathcal{M}_{N \to B}|^2 \, d\sigma_{MN \to \pi N}(s', t'). \quad (59)$$

We take the z axis as the momentum direction of the initial nucleon b, so that our momentum assignment for p_a, p_b, and p_e is

$$\begin{aligned} p_a &= (m_N, 0, 0, 0), \\ p_b &= (E_N, 0, 0, p_N), \\ p_e &= (E_B, p_B \sin\theta_e \cos\phi_e, p_B \sin\theta_e \sin\phi_e, p_B \cos\theta_e), \end{aligned} \quad (60)$$

where θ_e and ϕ_e are the polar and azimuthal angles for the baryon B. The integral over the B momentum $\vec{p}_e$ is written as

$$d^3 p_e = p_e^2 dp_e d\Omega_e = p_e^2 dp_e d(\cos\theta_e) d\phi_e, \quad (61)$$

The differential cross section for $NN \to N\pi B$ is expressed with respect to the kinematical variables t, t', y, ϕ_d, and ϕ_e, where the variable y is defined by

$$y \equiv \frac{s'}{s} = \frac{t + m_N^2 + 2(m_N E_N - E_B E_N + p_B p_N \cos\theta_e)}{s}. \quad (62)$$

The variable ϕ_d is the azimuthal angle for the final nucleon (d). Then, integrating over y, ϕ_d, and ϕ_e, we finally obtain the following differential cross section:

$$\frac{d\sigma_{NN \to N\pi B}}{dt \, dt'} = \int_{y_{min}}^{y_{max}} dy \; \frac{s}{16 \, (2\pi)^2 \, m_N \, p_N} \times \sqrt{\frac{(ys - t - m_N^2)^2 - 4m_N^2 t}{(s - 2m_N^2)^2 - 4m_N^4}} \; \frac{d\sigma_{MN \to \pi N}(s' = ys, t')}{dt'} \times \sum_{\lambda_a, \, \lambda_e} \frac{1}{[\phi_M(z)]^2} |\mathcal{M}_{N \to B}|^2, \quad (63)$$

where y_{max} and y_{min} are upper and lower bounds of the integral. From Eq. (62), y_{max} is obtained by taking $\cos\theta_e = 1$. The lower bound is estimated by applying a hard kinematical condition for t' and u': $|t'|$, $|u'| \geq Q_0^2$, where the hard scale is taken in the region Q_0^2=2∼3 GeV^2. The relation $s' + t' + u' = t + 2m_N^2 + m_\pi^2$ leads to

$$y_{min} = \frac{Q_0^2 + 2m_N^2 - t'}{s}, \quad -t' \geq Q_0^2, \quad (64)$$

where $|t|$, $m_\pi^2 \ll m_N^2$ is assumed.

We specify all used kinematical variables and constants. The initial proton energy is given by

$$E_N = m_N + T_N, \quad (65)$$

where the kinetic energy of the proton beam (T_N) is, for example, 30 GeV at the initial stage of J-PARC and is expected to be 50 GeV at the later stage. Then, the c.m. energy squared is calculated as

$$s = 2m_N^2 + 2m_N E_N, \quad (66)$$

The momentum transfer squared t is defined in Eq. (2) and we present the cross section as a function of this variable in Eq. (63). The value of t determines the energy and momentum of the final baryon B:

$$E_B = \frac{m_N^2 + m_B^2 - t}{2m_N}, \quad p_B = \sqrt{E_B^2 - m_B^2}, \quad (67)$$

in the rest frame of the nucleon (a). The polar angle of $\vec{p}_B$ is given by

$$\cos\theta_e = \frac{ys - t - m_N^2 + 2(E_B - m_N)E_N}{2 \, p_B \, p_N}. \quad (68)$$

In calculating the skewdness parameter ξ, we should be careful about the reaction kinematics. We consider a reaction by taking z axis along the incident proton beam, and the GPDs of a target hadron at rest are studied. In the c.m. frame, the target momentum along the z axis is negative. Therefore, the appropriate choice of the vector n^μ should be n_+^μ instead of the usual n_-^μ in many GPD articles:

$$n^\mu \equiv n_+^\mu = \left(\frac{1}{\sqrt{2}P^-}, \; 0, \; 0, \; \frac{1}{\sqrt{2}P^-} \right). \quad (69)$$

The skewdness parameter ξ becomes

$$\xi = -\frac{1}{2} n \cdot \Delta = \frac{m_N - E_B + p_B \cos\theta_e}{m_N + E_B - p_B \cos\theta_e}, \quad (70)$$

by using $\Delta = p_e - p_a$ and Eq. (60). Substituting Eq. (68) into this expression, we obtain

$$\xi = -\frac{ys - t - m_N^2 + 2(E_B - m_N)(E_N - p_N)}{ys - t - m_N^2 + 2(E_B - m_N)E_N - 2(E_B + m_N)p_N}. \quad (71)$$

The kinematical minimum ξ_{min} is calculated by substituting y_{min} into the above equation, whereas the maximum ξ_{max} is obtained by Eq. (70) with $\cos\theta_e = 1$.

Here, it should be noted that the energy and momentum of B depend on the variable t as explicitly shown in Eq. (67). The relation between ξ and y is obtained from Eqs. (62) and (70):

$$y = \frac{1}{s} \left[t + m_N^2 - 2(E_N - p_N) \, E_B + 2m_N E_N - 2\frac{1 - \xi}{1 + \xi} m_N \, p_N \right], \quad (72)$$

which will be used in changing the variable y for ξ when presenting the numerical results for the cross section in Sec. VI C.

The elastic scattering factor $d\sigma_{MN\to\pi N}(s',t')/dt'$ is calculated by using the result in Sec. V B, in particular Eq. (57) together with the parameter values in Table I. The last ingredient is the matrix elements $M_{N\to B}$ which are expressed by the GPDs. To be specific, we use Eqs. (32), (33), and (34) for calculating $\sum_{\lambda_N,\lambda_{N'}}|\mathcal{M}_N|^2$. The $N\to\Delta$ matrix element $\sum_{\lambda_N,\lambda_\Delta}|\mathcal{M}_{N\to\Delta}|^2$ is calculated by using Eqs. (35), (39), (40), (42), (43), (44), and (45). As we explain in the following subsection, in our numerical analysis we estimate the meson-pole contributions to the cross sections. The meson-pole contributions to the GPDs contain the meson wave function $\phi_M(z)$, which is divided out from the cross-section expression in Eq. (63). Therefore, a specific functional form of $\phi_M(z)$ is not necessary for our current numerical estimates.

B. Contributions from the meson poles

In this article we want to provide *first estimate of the order of magnitude for the $N+N\to N+\pi+B$ cross sections in order to establish feasibility of investigating the GPDs at hadron experimental facilities.* For this purpose, we employ a very simple description by meson poles. Our studies should be intended merely to provide a starting point for future theoretical and experimental studies.

In the ERBL region, major contributions to the GPDs come from meson poles, particularly the pion and ρ-meson poles, at small $|t|$. For numerical evaluations of the $N+N\to B+\pi+N$ cross sections, we show explicit expressions for these pole contributions to the nucleonic and $N\to\Delta$ transition GPDs.

First, the pion is a pseudo-scalar particle, so that it is related to the axial part of the nucleonic matrix element. The pion pole contributes only to the nucleonic GPD $\widetilde{E}(x,\xi,t)$ as [10, 49]

$$\widetilde{E}(x,\xi,t)=\frac{4\,g_A\,m_N^2}{1-t/m_\pi^2}\frac{\sqrt{3}}{m_\pi^2\,f_\pi\,\xi}\,\phi_\pi(z)\,\theta(\xi-|x|),\quad(73)$$

where g_A is the axial charge of the nucleon and its value is $g_A=1.2695$ [58]. Here, $\widetilde{E}$ indicates the isovector combination $\widetilde{E}^u-\widetilde{E}^d$. In the same way, ρ contributions can be estimated. Since the ρ is a vector particle, it contributes to the vector part of the matrix element. The ρ-pole terms are given by extending the expression in Ref. [59]:

$$\begin{aligned}H(x,\xi,t)&=\frac{1}{1-t/m_\rho^2}\,\frac{C_1}{g_\rho}\frac{\sqrt{3}}{\sqrt{2}\,f_\rho\,\xi}\,\phi_\rho(z)\,\theta(\xi-|x|),\\ E(x,\xi,t)&=\frac{1}{1-t/m_\rho^2}\,\frac{C_2}{g_\rho}\frac{\sqrt{3}}{\sqrt{2}\,f_\rho\,\xi}\,\phi_\rho(z)\,\theta(\xi-|x|),\quad(74)\end{aligned}$$

where the C_1 and C_2 are two-types of ρ coupling constants with the nucleon, and they are given for the isovector couplings, namely for the isovector ρ, by

$$\frac{C_1}{g_\rho}=\frac{e_p-e_n}{2}=\frac{1}{2},\quad\frac{C_2}{g_\rho}=\frac{\kappa_p-\kappa_n}{2\cdot 2m_N}=\frac{1.85295}{2m_N},\quad(75)$$

where e_p (e_n) is the charge of the proton (neutron) and κ_p (κ_n) is the anomalous magnetic moment of the proton (neutron) [58]. There is no pion contribution to $\widetilde{H}(x,\xi,t)$ because the function $\widetilde{H}$ is chiral even, whereas the pion should contribute to the chiral odd.

We may note that normalizations of the pion and ρ wave functions are given by

$$\begin{aligned}1&=\int_{-1}^{1}dx\,\theta(\xi-|x|)\,\frac{\sqrt{3}}{f_\pi\,\xi}\,\phi_\pi(z)\\ &=\int_{-1}^{1}dx\,\theta(\xi-|x|)\,\frac{\sqrt{3}}{\sqrt{2}\,f_\rho\,\xi}\,\phi_\rho(z),\quad(76)\end{aligned}$$

where the normalization factors are slightly different from the ones in Ref. [10].

As for the light-cone wave function of the meson M, we may take, for example, asymptotic wave function of pion and ρ mesons [55, 56]:

$$\begin{aligned}\phi_\pi(z)&=\sqrt{3}f_\pi z(1-z),\\ \phi_\rho(z)&=\sqrt{6}f_\rho z(1-z).\quad(77)\end{aligned}$$

The normalization of these wave function is uniquely fixed in QCD [55, 56]. For the pion wave function it is given by

$$\int dz\phi_\pi(z)=\int\frac{dz\,d^2k_\perp}{16\pi^3}\psi_\pi(z,\vec{k}_\perp)=\frac{f_\pi}{2\sqrt{3}},\quad(78)$$

where f_π is the pion decay constant for $\pi^+\to\mu^+\nu_\mu$. By noting the difference of $\sqrt{2}$ from the value in Ref. [58, 60], it is f_π=92.4 MeV. The ρ decay constant f_ρ is determined by the decay $\rho^0\to e^+e^-$, and it is given by [56, 58]

$$f_\rho=\sqrt{\frac{3m_\rho\Gamma_{\rho^0\to e^+e^-}}{8\pi\alpha^2}}=110.6\text{ MeV}.\quad(79)$$

where m_ρ is the ρ mass, α is the fine structure constant, and $\Gamma_{\rho^0\to e^+e^-}$ is the $\rho^0\to e^+e^-$ decay width.

Next, pion and ρ contributions are shown for the $N\to\Delta$ transition GPDs. The pion contributes to the axial part, particularly the GPD $\widetilde{H}_2$ [10, 48], is given in the same way by

$$\widetilde{H}_2(x,\xi,t)=\frac{3\,g_A\,m_N^2}{(1-t/m_\pi^2)\,m_\pi^2\,\xi\,f_\pi}\,\phi_\pi(z)\,\theta(\xi-|x|).\quad(80)$$

The ρ-meson contribution to the vector part is expressed by the magnetic $N\to\Delta$ transition as

$$H_M(x,\xi,t)=\frac{G_M^*}{1-t/m_\rho^2}\,\frac{\sqrt{3}}{\sqrt{2}\,f_\rho\,\xi}\,\phi_\rho(z)\,\theta(\xi-|x|),\quad(81)$$

where G_M^* is the transition magnetic moment [45]. Experimental measurements indicate $G_M^* \approx 3$ [50], which is close to an expectation $G_M^* = (\mu_p - \mu_n)/\sqrt{2} = 3.32757$ [10], where μ_p and μ_n are magnetic moments for the proton and the neutron, respectively. In our numerical analysis, we use the value $G_M^* = 3.3$ for the transition magnetic moment.

C. Numerical results

From measurements of the $N + N \to B + \pi + N$ cross sections, the GPDs should be extracted from the data. There is no such data at this stage, so that we need to provide an order of magnitude estimates of the cross sections for experimental proposals at hadron experimental facilities, for example, J-PARC and GSI-FAIR [28, 29]. Since large contributions should come from pion- and ρ-pole terms, such pole contributions are evaluated in this work. However, one should note that the following numerical evaluations based on the meson-pole terms are just rough estimates of the cross sections. In particular, there exists an extra t dependence in the GPDs at large $|t|$ (like form factors at large $|t|$) in addition to the pole t-dependence, and it is neglected in this work. Conversely, the actual GPDs need to be extracted from future measurements once the data are taken. Then, they should be used for investigating the spin structure of the nucleon, especially orbital angular momentum effects, and electromagnetic properties of the $N \to \Delta$ transition as explained in Sec. III B and Sec. III C.

In the case when incident particles are unpolarized and polarization of the final particles is averaged over, we predict the same cross section for analogous reactions initiated by antiprotons. Interference of axial and vector terms survives if the target proton is transversely polarized. Interestingly, the sign of the interference effect for incident protons and antiprotons depends on relative phase of the $A_{\pi N \to \pi N}$ and $A_{\rho N \to \pi N}$ amplitudes. In leading QCD, diagrams for this process correspond to real amplitudes, so the relative phase could be either 1 or -1. So, in principle, by combining measurements with proton and antiproton beams, one can measure this phase.

We show the numerical results for the following three cross sections

(1) $p + p \to p + \pi^+ + \Delta^0$,

(2) $p + p \to p + \pi^- + \Delta^{++}$,

(3) $p + p \to p + \pi^+ + n$,

in Fig. 11 for the kinetic energy of the proton beam at 30 and 50 GeV. We focus on these processes for several reasons: they are among the simplest to measure experimentally, they are expressed through the GPDs which are best studied theoretically, and they are expressed through elementary large angle meson-nucleon reactions which were studied experimentally.

Also, in these processes the intermediate state with the vacuum quantum number 0^+ does not contribute as explained in Sec. II which further simplifies the description. The cross sections are calculated at the momentum transfer $t = -0.3$ GeV^2, and the momentum cutoff in Eq. (64) is taken as Q_0^2=3 GeV^2. The cross sections are decreasing function of $-t'$, and they are of the order of $\mu\,$barn/GeV^2. Hence it appears feasible to accumulate large statistics for these reactions over the range of t' for several incident energies and check the suggested mechanism of the reaction. Therefore it should be in principle possible to measure the GPDs in the $N+N \to N+\pi^+ +B$ reactions. The Δ-production cross sections are as large as the nucleonic one, which indicates that $N \to \Delta$ transition GPDs could be also studied as well as the nucleonic GPDs. At $T_N = 50$ GeV, the magnitude of the cross sections becomes slightly smaller; however, the larger beam energy is valuable for extending the kinematical region of t (and ξ as shown later) and testing the mechanism of the reaction in particular by comparing the cross sections for the same s', t' and different E_N.

Next, the pion and ρ-meson contributions to the cross sections are explicitly shown for the processes $p + p \to p + \pi^+ + n$ and $p + p \to p + \pi^+ + \Delta^0$ in Fig. 12 at the 30

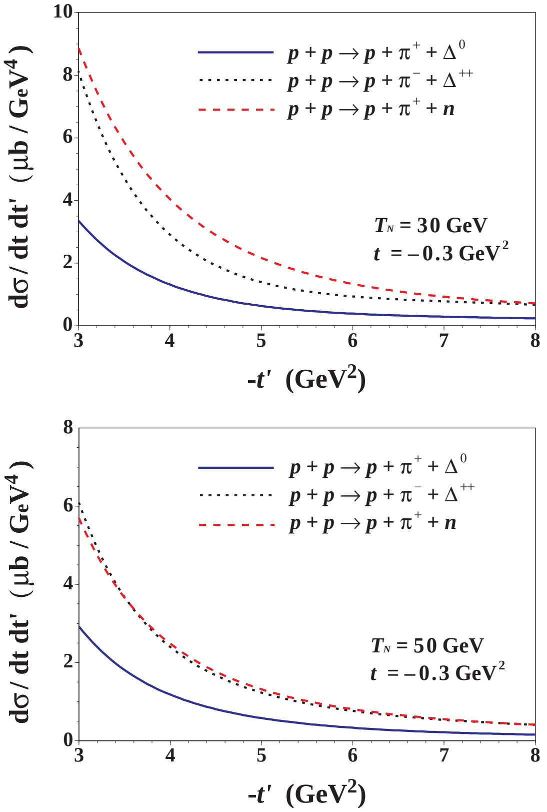

FIG. 11: Differential cross section as a function of t'. The incident proton-beam energy is 30 (50) GeV in the upper (lower) figure, and the momentum transfer is $t = -0.3$ GeV^2. The solid, dotted, and dashed curves indicate the cross sections for $p + p \to p + \pi^+ + \Delta^0$, $p + p \to p + \pi^- + \Delta^{++}$, and $p + p \to p + \pi^+ + n$, respectively.

GeV beam energy and the momentum transfer $t = -0.3$ GeV^2. The results indicate that the contribution from the ρ-like vector GPD terms are smaller than the pion-like axial-vector terms in both process $p+p \to p+\pi^+ +n$ and $p+p \to p+\pi^+ + \Delta^0$. Especially at large $-t'$, the ρ contributions are much smaller than the pion ones. It is expected in general because cross sections should be suppressed for heavier-meson intermediate states. Therefore, it is important first to understand the axial-vector (quark spin independent) GPDs for estimating the magnitude of the cross sections. However, both the axial-vector and vector (spin dependent) GPDs should be calculated for estimating the cross sections. Once experimental data are obtained, they should be valuable for determining both spin independent and spin dependent GPDs for the nucleon and for the $N \to \Delta$ transition.

The cross-section results are presented in Figs. 11 and 12 for the hard momentum cutoff Q_0^2=3 GeV^2 for t' and u' in Eq. (64). We show the cutoff dependence of the cross sections in Fig. 13 within the range 2 GeV$^2 \le Q_0^2 \le$ 4 GeV^2. The cross sections depend strongly on the cutoff if it is taken low enough $\sim$ 2 GeV^2. As the momentum transfers $|t'|$ and $|u'|$ become smaller, soft contributions become larger. It will be important to study process as a function of $-t'$ to determine minimal value of the cutoff which is necessary for using discussed hadronic processes for determination of the nucleonic and $N \to \Delta$ transition GPDs.

In connection with the studies of GPDs, it is instructive to present the cross sections as a function of ξ without integrating them over the variable y. Using the relation between the variables y and ξ in Eq. (72), we calculate the differential cross sections $d\sigma/d\xi dt dt'$. In Fig. 14, the cross sections are shown as a function

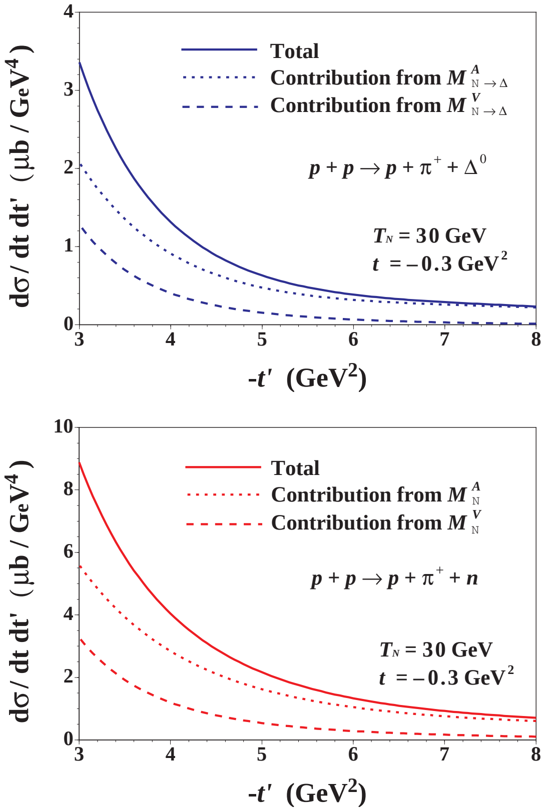

FIG. 12: Differential cross section as a function of t'. The incident proton-beam energy is 30 GeV, and the momentum transfer is $t = -0.3$ GeV^2. The upper (lower) figure indicates the cross section for the process $p+p \to p+\pi^+ + \Delta^0$ ($p+p \to p+\pi^+ + n$). The solid, dotted, and dashed curves indicate the cross sections for the total, axial-vector (π) contribution, vector (ρ) contribution, respectively.

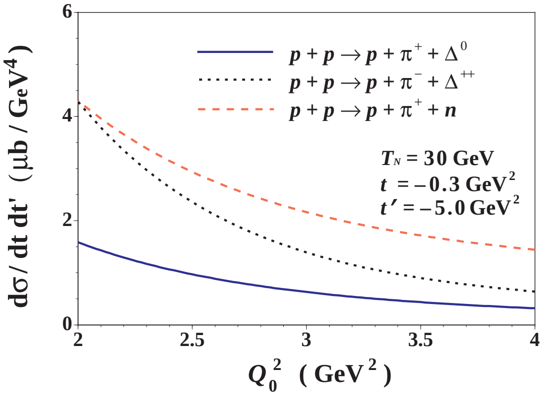

FIG. 13: Cutoff (Q_0^2) dependence of differential cross section. The incident proton-beam energy is 30 GeV, and momentum transfers are fixed at $t = -0.3$ GeV^2 and $t' = -5$ GeV^2. The solid, dotted, dashed curves indicate the cross sections for $p+p \to p+\pi^+ + \Delta^0$, $p+p \to p+\pi^- + \Delta^{++}$, and $p+p \to p+\pi^+ + n$, respectively.

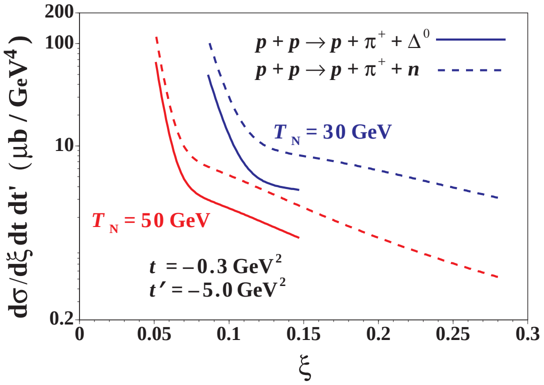

FIG. 14: Differential cross sections are shown as a function of ξ at the incident proton-beam energy 30 (or 50) GeV, $t = -0.3$ GeV^2, and $t' = -5$ GeV^2. The solid and dashed curves indicate the cross sections for $p+p \to p+\pi^+ + \Delta^0$ and $p+p \to p+\pi^+ + n$, respectively. The two upper (lower) curves indicate the cross sections at $T_N = 30$ (50) GeV. There is a restriction on the kinematical range, $\xi_{min} < \xi < \xi_{max}$, which is explained in the text.

of ξ at fixed t and t' ($t = -0.3$ GeV^2 and $t' = -5$ GeV^2). It should be noted that the kinematical range of ξ is limited ($\xi_{min} < \xi < \xi_{max}$) as explained below Eq. (71). The minimum ξ_{min} comes from the hard kinematical condition for $|t'|$ and $|u'|$, and the minimum ξ_{min} is due to the minimum polar angle for the final baryon B ($\theta_e = 0$). Because of the larger masses for the Δ than the one for the nucleon, the ξ range is more restricted: $\xi_{max} = (m_N - E_B + p_B)/(m_N + E_B - p_B)$ for the Δ. At larger beam energy ($T_N = 50$ GeV), the smaller-ξ region is probed by the reactions. Therefore, 50-GeV experiments are valuable for extending the kinematical regions (in ξ and also t) of the GPD measurements in addition to the 30-GeV experiments. Note in passing that the use of 50 GeV proton beam would allow to produce secondary beams of mesons and perform precision measurements of meson-nucleon large angle scattering processes which enter in the analysis of the $2 \to 3$ processes and of interest on their own.

Next, the same cross sections are calculated at different momentum transfer points for t. At a given ξ, there is a restriction for the variable t at $\theta_e = 0$, and it is given by $(-t)_{min} = 2\xi[m_B^2/(1-\xi) - m_N^2/(1+\xi)]$. The cross sections are calculated at this point of t for each ξ in Fig. 15. Then, the cross-section range is extended to larger ξ. Measuring these cross sections at future facilities at J-PARC and GSI-FAIR, we should be able to obtain information on the GPDs in the ERBL region.

In this article, we discussed processes $N + N \to N + \pi + B$ (B=N or Δ) for investigating the GPDs at the hadron facilities. In addition to these GPD studies for the nucleon and Δ, strange-particle productions are also quite interesting, and they can be calculated along the same line. For example, the process $p + p \to \Lambda + p + K^+$ is likely to have a cross section comparable to that of the reactions we discussed in this work as the smaller $K\Lambda N$ vertex is to some extent compensated by larger cross section of $K^+p \to K^+p$ scattering.

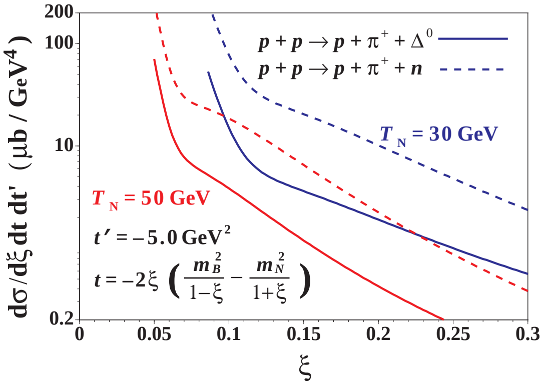

FIG. 15: Differential cross sections are shown as a function of ξ at the incident proton beam energy is 30 (or 50) GeV and $t' = -5$ GeV^2. The notations are the same in Fig. 14. The momentum transfer t is taken at $\cos\theta_e = 1$ as a function of ξ.

VII. SUMMARY

We introduced a new class of hard $2 \to 3$ branching hadronic processes and investigated a possibility that the generalized parton distributions for the nucleon and the $N \to \Delta$ transition could be investigated in the reaction $N + N \to N + \pi + B$ where B is the nucleon or Δ. First, we argued that the process is factorized into two blocks, $N \to B$ and meson-nucleon (MN) scattering by imposing hard scattering condition for the meson-nucleon block. The $N \to B$ part is expressed in terms of the nucleonic and the $N \to \Delta$ transition GPDs, and the MN scattering part is parametrized so as to explain the experimental elastic scattering cross sections. The GPDs can be studied in the ERBL region by such exclusive reactions.

Using the meson-pole model for the GPDs, we estimated the magnitude of the cross section of several reactions $pp \to p\pi N(\Delta)$. We found a cross sections are in the range measurable at the high-energy hadron facilities. Experimental studies will be possible in two kinematics: one corresponding to the baryon B been slow in the rest frame, and another when B originates from the projectile (cross sections for the two kinematics are equal and we presented only one in our plots). Experimental investigations in the first kinematics would require both forward and recoil detectors, while in the second kinematics a forward multiparticle detector may be sufficient. Our results indicate that both the nucleonic and the $N \to \Delta$ transition GPDs could be measured in hadron reactions. Future high-energy hadron facilities such as J-PARC and GSI-FAIR will provide opportunities to investigate various interesting aspects of the GPDs in a way complementary to the measurements using lepton scattering. These measurements will be valuable for finding the origin of the nucleon spin, especially on the orbital-angular-momentum contribution. Note that the studied GPDs probe the isovector part of the quark angular momenta both in the $p \to n$ and $N \to \Delta$ channels.

Acknowledgments

The authors thank M. V. Polyakov, S. Sawada, and M. Vanderhaeghen for valuable suggestions and comments. This research has been partially supported by the Research Program of Hayama Center for Advanced Studies of Sokendai and by the US DOE Contract Number DE-FG02-93ER40771. MS would like to thank KEK for hospitality during the visit when this project has started.

---

[1] For a review, see J. C. Collins, D. E. Soper, and G. Sterman, Adv. Ser. Direct. High Energy Phys. **5**, 1 (1988) [arXiv:hep-ph/0409313].

[2] For a recent situation, see S. E. Kuhn, J.-P. Chen, and E. Leader, arXiv:0812.3535 [hep-ph]. to be published in Progress in Particle and Nuclear Physics; M. Hirai and S. Kumano, Nucl. Phys. B **813**, 106 (2009).

[3] A. Airapetian *et al.* (HERMES Collaboration), Phys. Rev. Lett. **84**, 2584 (2000); B. Adeva *et al.* (Spin Muon Collaboration (SMC)), Phys. Rev. D **70**, 012002 (2004); A. Adare *et al.* (PHENIX collaboration), Phys. Rev. D **76**, 051106 (2007).

[4] D. Muller *et al.*, Fortsch. Phys. **42**, 101 (1994); X.-D. Ji, Phys. Rev. D **55**, 7114 (1997); A. V. Radyushkin, Phys. Rev. D **56**, 5524 (1997); J. J. Collins and A. Freund, Phys. Rev. D **59**, 074009 (1999).

[5] S. J. Brodsky, L. Frankfurt, J. F. Gunion, A. H. Mueller, and M. Strikman, Phys. Rev. D **50**, 3134 (1994).

[6] J. C. Collins, L. Frankfurt, and M. Strikman, arXiv: hep-ph/9709336.

[7] M. Burkardt, Phys. Rev. D **62**, 071503 (2000); **66**, 119903 (2002) (errattum); M. Diehl, Eur. Phys. J. C **25**, 223 (2002); **31**, 277 (2003) (erratum); J. P. Ralston and B. Pire, Phys. Rev. D **66**, 111501 (2002).

[8] For a review, see L. Frankfurt, M. Strikman, and C. Weiss, Ann. Rev. Nucl. Part. Sci. **55**, 403 (2005).

[9] X.-D. Ji, Phys. Rev. Lett. **78**, 610 (1997); Ann. Rev. Nucl. Part. Sci. **54**, 413 (2004).

[10] K. Goeke, M. V. Polyakov, and M. Vanderhaeghen, Prog. Part. Nucl. Phys. **47**, 401 (2001).

[11] M. Diehl, Phys. Rept. **388**, 41 (2003); A. V. Belitsky and A. V. Radyushkin, Phys. Rept. **418**, 1 (2005).

[12] J. Ossmann, M.V. Polyakov, P. Schweitzer, D. Urbano, and K. Goeke, Phys. Rev. D **71**, 034011 (2005).

[13] M. Wakamatsu and H. Tsujimoto, Phys. Rev. D **71**, 074001 (2005); M. Wakamatsu, Phys. Rev. D **72**, 074006 (2005); **79**, 014033 (2009); M. Wakamatsu and Y. Nakakoji, Phys. Rev. D **74**, 054006 (2006).

[14] M. Dorati, T. A. Gail, and T. R. Hemmert, Nucl. Phys. A **798**, 96 (2008).

[15] D. Brommel *et al.*, (QCDSF-UKQCD Collaboration), PoS LAT2007, 158 (2007); P. Hagler *et al.* (LHPC Collaboration), Phys. Rev. D **77**, 094502 (2008).

[16] A. Freund, M. McDermott, and M. Strikman, Phys. Rev. D **67**, 036001 (2003).

[17] S. Ahmad, H. Honkanen, S. Liuti, and S. K. Taneja, Phys. Rev. D **75**, 094003 (2007); O. V. Selyugin and O. V. Teryaev, Phys. Rev. D **79**, 033003 (2009).

[18] S. Chen *et al.* (CLAS Collaboration), Phys. Rev. Lett. **97**, 072002 (2006); F. H. Heinsius (COMPASS Collaboration), pp. 1121-1124 in Proceedings of the 5th International Workshop on Deep-Inelastic Scattering and Related Subjects (2007).

[19] Recent studies are explained in M. Guidal, Prog. Part. Nucl. Phys. **61**, 89 (2008); C. Weiss, arXiv:0902.2018 [hep-ph].

[20] E. R. Berger, M. Diehl, and B. Pire, Phys. Lett. B **523**, 265 (2001).

[21] L. L. Frankfurt, M. V. Polyakov, and M. Strikman, hep-ph/9808449; L. L. Frankfurt, M. V. Polyakov, M. Strikman, and M. Vanderhaeghen, Phys. Rev. Lett. **84**, 2589 (2000).

[22] D. Drechsel and T. Walcher, Rev. Mod. Phys. **80**, 731 (2008); B. Krusche and S. Schadmand, Prog. Part. Nucl. Phys. **51**, 399 (2003).

[23] L. Heller, S. Kumano, J. C. Martinez, and E. J. Moniz, Phys. Rev. C **35**, 718 (1987); A. Bosshard *et al.*, Phys. Rev. D **44**, 1962 (1991).

[24] B. Julia-Diaz, T.-S. H. Lee, T. Sato, and L. C. Smith, Phys. Rev. C **75**, 015205 (2007); A. I. Machavariani and A. Faessler, Phys. Rev. C **72**, 024002 (2005); A. J. Buchmann, J. A. Hester, R. F. Lebed, Phys. Rev. D **66**, 056002 (2002); S. Kumano, Phys. Lett. B **214**, 132 (1988); Nucl. Phys. A **495**, 611 (1989).

[25] M. I. Strikman and L. L. Frankfurt, pp. 211-220 in Proceedings of the 7th International Conference on the Structure of Baryons (1995); M. Strikman and M. Zhalov, Nucl. Phys. A **670**, 135 (2000).

[26] L. Frankfurt, M. V. Polyakov, M. Strikman, D. Zhalov, and M. Zhalov, arXiv:hep-ph/0211263, pp. 361-368 in Proceedings of of Exclusive Processes at High Momentum Transfer, Newport News, Virginia, 15-18 May 2002.

[27] A. V. Efremov and A.V. Radyushkin, Phys. Lett. B **94**, 245 (1980); G. P. Lepage and S. J. Brodsky, Phys. Lett. B **87**, 359 (1979).

[28] The J-PARC project is found http://j-parc.jp/index-e.html; S. Sawada, Nucl. Phys. A **782**, 434 (2007); S. Kumano, Nucl. Phys. A **782**, 442 (2007).

[29] http://www.gsi.de/fair/index_e.html.

[30] D. Zhalov *et al.* (E850 Collaboration), AIP Conf. Proc. **549**, 310 (2002); D. Zhalov, Ph. D. Thesis (report UMI-30-36627), Pennsylvania State University (2001).

[31] S. J. Brodsky and G. R. Farrar, Phys. Rev. Lett. **31**, 1153 (1973); Phys. Rev. D **11**, 1309 (1975).

[32] C. White *et al.*, Phys. Rev. D **49**, 58 (1994).

[33] A. H. Mueller, p.13 in Proceedings of 17th rencontre de Moriond, edited by J. Tran Thanh Van (Editions Frontieres, Gif-sur-Yvette, France, 1982) Vol. I.

[34] S. J. Brodsky, p.963 in Proceedings of the 13th International Symposium on Multiparticle Dynamics, edited by W. Kittel, W. Metzger, and A. Stergiou (World Scientific, Singapore 1982).

[35] L. L. Frankfurt, G. A. Miller, and M. Strikman, Ann. Rev. Nucl. Part. Sci. **44**, 501 (1994).

[36] B. Clasie *et al.*, Phys. Rev. Lett. **99**, 242502 (2007).

[37] A. Larson, G. A. Miller, and M. Strikman, Phys. Rev. C **74**, 018201 (2006).

[38] C. E. Carlson, J. R. Hiller, and R. J. Holt, Ann. Rev. Nucl. Part. Sci. **47**, 395 (1997).

[39] For example, see Y. Chen *et al.*, Phys. Rev. D **73**, 014516 (2006).

[40] K.-C. Yang, Nucl. Phys. B **776**, 187 (2007).

[41] F. E. Close and N. A. Törnqvist, J. Phys. **G28**, R249 (2002); F. E. Close, N. Isgur, and S. Kumano, Nucl. Phys. **B389**, 513 (1993); M. Hirai, S. Kumano, M. Oka, and K. Sudoh, Phys. Rev. D **77**, 017504 (2008).

[42] A. R. Edmonds, *Angular Momentum in Quantum Mechanics* (Princeton University Press, 1974); S. Kumano, Phys. Rev. D **41**, 195 (1990).

[43] The definition of n^μ is taken from Ref. [10] and it is different from the one in Ref. [11], where $n_-^\mu =$

$(1,0,0,-1)/\sqrt{2}$. The definition of other variables, P, Δ, and ξ are the same in both articles.

[44] In our actual calculations in Sec .VI, a different one (n_+^μ) is used by considering $(p_a)_z < 0$ in the c.m. frame of initial nucleons a and b. The details are explained in Sec. VI.

[45] H. F. Jones and M. D. Scadron, Ann. of Phys. **81**, 1 (1973).

[46] J. D. Bjorken and S. D. Drell, *Relativistic Quantum Fields* (McGraw-Hill, Inc., 1965).

[47] S. Gasiorowicz, *Elementary Particle Physics* (Jone Wiley & Sons, Inc., 1966); D. Lurié, *Particles and Fields* (Jone Wiley & Sons, Inc., 1968).

[48] We denoted the spin-dependent $N \to \Delta$ transition GPDs as $\widetilde{H}_i(x,\xi,t)$ instead of $C_i(x,\xi,t)$ in Refs. [10, 21] throughout this article in order to use similar notations to the nucleonic ones.

[49] M. Penttinen, M. V. Polyakov, and K. Goeke, Phys. Rev. D **62**, 014024 (2000).

[50] M. Ungaro, K. Joo, and P. Stoler, in *Shapes of Hadrons*, edited by C. N. Papanicolas and A. M. Bernstein, AIP Conf. Proc. **904**, 232 (2007).

[51] S. L. Adler, Ann. Phys. **50**, 189 (1968); Phys. Rev. D **12**, 2644 (1975).

[52] N. C. Mukhopadhyay *et al.*, Nucl. Phys. **A633**, 481 (1998); K. A. Aniol *et al.* (HAPPEX Collaboration), Phys. Rev. C **69**, 065501 (2004); C. Alexandrou, T. Leontiou, J. W. Negele, Phys. Rev. Lett. **98**, 052003 (2007).

[53] L. S. Geng, J. Martin Camalich, L. Alvarez-Ruso, and M. J. Vicente Vacas, Phys. Rev. D **78**, 014011 (2008).

[54] L. L. Frankfurt, L. Mankiewicz, and M. I. Strikman, Z. Phys. A **334**, 343 (1989); S. Kumano, Phys. Rev. D **43**, 59 (1991); 3067 (1991); Phys. Rept. **303**, 183 (1998); S. Kumano and J. T. Londergan, Phys. Rev. D **44**, 717 (1991).

[55] G. P. Lepage and S. J. Brodsky, Phys. Lett. B **87**, 359 (1979); S. J. Brodsky, T. Huang, and G. P. Lepage, report SLAC-PUB-2540 (1980); T. Huang, B.-Q. Ma, and Q.-X. Shen, Phys. Rev. D **49**, 1490 (1994).

[56] S. J. Brodsky *et al.*, Phys. Rev. D **50**, 3134 (1994).

[57] G. C. Blazey *et al.*, Phys. Rev. Lett. **55**, 1820 (1985); B. R. Baller *et al.*, Phys. Rev. Lett. **60**, 1118 (1988).

[58] C. Amsler *et al.* (Particle Data Group), Phys. Lett. B **667**, 1 (2008).

[59] R. P. Feynman, p.91 in *Photon-Hadron Interactions* (W. A. Benjamin, Inc., 1972).

[60] Review of Particle Physics 2006 Edition, http://ccwww.kek.jp/pdg/2006/pdg_2006.html.